N O T I C E

THIS DOCUMENT HAS BEEN REPRODUCED FROM
MICROFICHE. ALTHOUGH IT IS RECOGNIZED THAT
CERTAIN PORTIONS ARE ILLEGIBLE, IT IS BEING RELEASED
IN THE INTEREST OF MAKING AVAILABLE AS MUCH
INFORMATION AS POSSIBLE

(NASA-CR-168416) CONTROL OF INTERFACE REACTIONS IN SIC/TI COMPOSITES Final Progress Report, Nov. 1977 - Jun. 1981 (Virginia Polytechnic Inst. and State Univ.) 61 p HC A04/MF A01 CSCL 11D G3/24
N82-17266
Unclas
08889

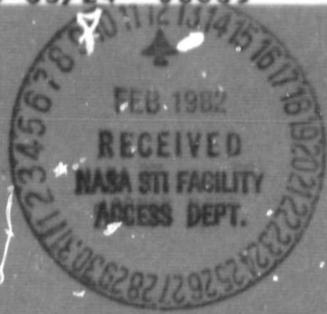

COLLEGE OF ENGINEERING

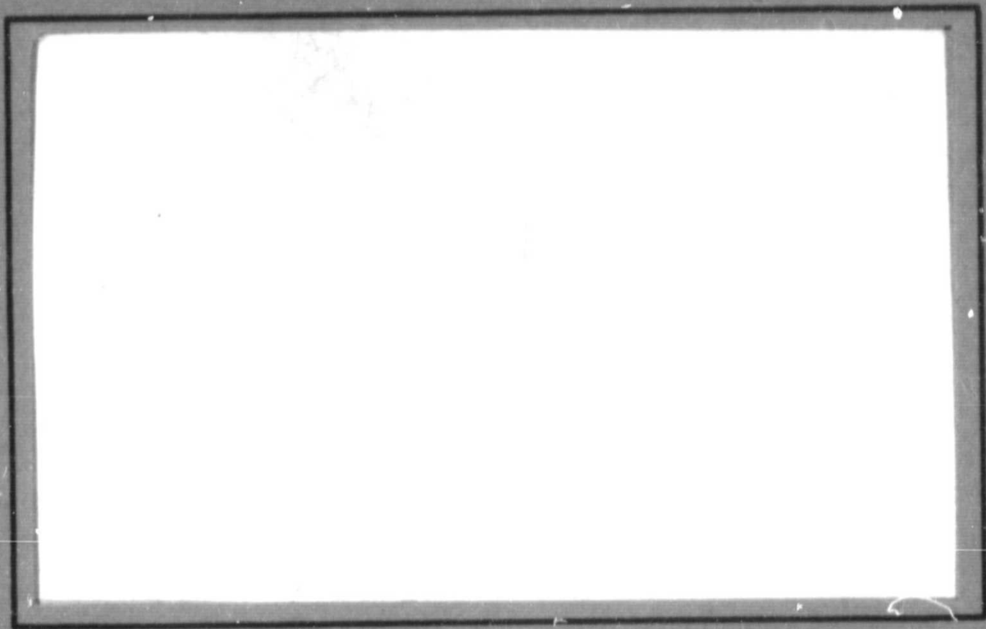

VIRGINIA POLYTECHNIC INSTITUTE AND STATE UNIVERSITY

BLACKSBURG, VIRGINIA

CONTROL OF INTERFACE REACTIONS

IN

SIC/TI COMPOSITES

C. R. Houska[+] and V. Rao[++]

Feb., 1982

Period: 11/77-6/81

Final Progress Report

NASA Grant NSG 1470

The NASA Technical Officer for this report is Dr. D. R. Tenney, NASA-Langley Research Center.

[+]Principal Investigator, Dept. of Materials Engineering, VPI&SU, Blacksburg, VA 24061.

[++]Research Associate.

CONTENTS

The following report (Parts I and II) is based largely upon the PhD dissertation of Dr. Venkatraman B. Rao at the Virginia Polytechnic Institute. This was completed Oct., 1980 as a requirement for the doctorate in Materials Engineering Science.

This final progress report prepared by the principal investigator is divided into three self contained parts:

I. GENERAL INTRODUCTION, INTERFACE REACTIONS IN PLANAR COMPOSITES.

II. REACTIONS AND DIFFUSION BETWEEN AN Al FILM AND A Ti SUBSTRATE.

III. REFINEMENTS ON THE X-RAY INTENSITIES FROM $Ti_{3-2}Al$. This is based, in part, upon the M.S. Thesis of Augusto Penaloza completed in June, 1981 at the Virginia Polytechnic Institute.

INTRODUCTION

Titanium matrix composites have not reached their full potential because of problems associated with instabilities at the fiber/matrix interface or loss of fiber strength at elevated temperatures. A more detailed understanding of the interfacial reaction kinetics and the behavior of the fiber are required if new processes and materials are to be developed for improving the high temperature stability of these materials.

Earlier work had indicated that the high temperature stability of SiC filaments could be effectively utilized in a Ti matrix composite.[1] Also the availability and lower cost of SiC filaments over either Boron or Borsic filaments could make SiC reinforced composites economically feasible. Consolidation subjects the composite to more severe conditions than what are normally anticipated during actual service. Therefore, a major limitation in the use of these composites relates to physical-chemical behavior of the SiC/Ti interface during fabrication.

An examination of the limited kinetic data in the literature dealing with the interfacial stability of SiC/Ti composites may lead one to conclude that they are incompatible. However, the same conclusion might have been made about the B/Al system before the concept of the protective interface was introduced.[2] Also, if solid rather than liquid fabrication techniques are used, a relatively stable interface is formed between a boron oxide film and the oxide on aluminum. These investigations are centered on finding a similar protective mechanism for SiC/Ti composites.

Two types of bonds are of importance for the SiC/Ti system.[2] These are reaction bonds associated with the compounds TiC, Ti_5Si_3 and $TiSi_2$,

and the "exchange reaction bond" in which a two stage reaction is believed to occur. Previous investigations[3,4] of the reactions between SiC and Ti or Ti or Ti alloys are based primarily on optical or scanning electron microscopy and electron microprobe data. Consequently, the early stages of the reaction, which are of considerable importance, have not received enough attention. Because of resolution limitations with the electron microprobe, quantitative data has only been obtained in the over reacted state, i.e. with reaction zones in excess of 1 micron, where the mechanical properties have already deteriorated. Special x-ray diffraction techniques are used in this investigation that allow smaller zones to be investigated.

The SiC reaction with Ti proceeds by the simultaneous recession of the filament and the growth of the reaction zone into Ti[5] without porosity. Interface motion was reported to be parabolic. Saturation of Ti with dissolved C increases the rate of transformation.[4] Before saturation, the Ti matrix acts as a sink for C atoms thereby removing this atom from the reaction zone.

Although some reaction at the interface is desirable, continued reaction to form a new compound beyond a maximum size is undesirable. At this point, the new compound at the interface can be more degrading to mechanical properties than simple solution. The compound is usually brittle and its strain to fracture is lower than the filament. Cracks may form if the reaction results in a reduction in the specific volume, which is usually the case.

It is known that silicide M_5Si_3 phases can greatly lower the Si flux. The following data at 1100°C (1373 °K) for the Mo-Si system[6] illustrates this point:

$$D_{MoSi_2} = 2.2\times10^{-5}\ cm^2\ sec^{-1}$$

$$D_{Mo_5Si_3} = 7.5\times10^{-7}\ cm^2\ sec^{-1}$$

$$D_{Mo} = 1.2\times10^{-4}\ cm^2\ sec^{-1}$$

All of the above diffusion coefficients (DC) refer to Si diffusion. If these data are normalized to the DC for Si diffusion in Mo, one finds

$$\frac{D_{MoSi_2}}{D_{Mo}} = 0.18 \qquad \frac{D_{Mo_5Si_3}}{D_{Mo}} = 6.1\times10^{-3}$$

indicating that the $MoSi_2$ phase is not much better as a barrier than pure Mo. However, the Mo_5Si_3 phase represents a barrier far superior to the other two. It has been found that W_5Si_3, Nb_5Si_3 and Ta_5Si_3 are even more effective barriers with Ta_5Si_3 being the most effective.[7] The M_5Si_3 silicides generally have the highest melting points. However, they are not always formed in thin film reactions between Si and M, indicating that although they are highly stable, the kinetics of formation are less favorable than for other silicides. The diffusion flux of metal atoms is much smaller than for Si in these compounds, and growth requires the transport of Si through the silicide to the silicide/metal interface.

A second interface control mechanism which appears to be understood in the B/Ti (Al) system could also play an analogous role for the SiC/Ti(Al) system. This is the exchange reaction bond which can be described by the following two step reaction beginning with a solid solution of Al in Ti:[2]

1. $Ti\ (Al)_{ss} + B = (Ti,\ Al)\ B_2$
2. $Ti + (Ti,\ Al)\ B_2 = Ti\ B_2 + Ti\ (Al)_{ss}$

The first reaction is governed by kinetic considerations and not by equilibrium thermodynamics. In the second reaction, the trend is toward thermodynamic equilibrium which results in the rejection of Al into the Ti(Al) matrix. When Al is rejected, the matrix adjacent to the diboride becomes enriched in Al and retards further transformation. The rate of growth therefore depends upon the rate of diffusion of Al away from the interface. Rejection of Al by the exchange reaction occurs in the system B/Ti-8Al-1Mo-1V. Exchange reactions should also be important in the SiC/Ti(Al) system since Al alone does not form silicides. The exchange reaction requires a second element such as either Al or Mo that form silicides of lower stability.

Schob, et al.[8] have reported that in the presence of aluminum, a C49 type orthorhombic Ti(Al)Si phase forms in preference to the C54 type $TiSi_2$ phase. The elevated temperature studies on Borsic/Ti-3Al-2.5V[4] confirmed the formation of large amounts of $TiSi_2$ (C54 type). The absence of the C49 type disilicide suggests that Al was being rejected from the reaction zone. The Al rejection mechanism has also been verified by electron microprobe data.[9]

SAMPLE PREPARATION

SiC/Ti composites containing a Mo_5Si_3 barrier film were investigated relative to the SiC/Ti interface without a barrier. Samples containing Al films sandwiched between SiC and Ti were used to investigate the effectiveness of Al as an exchange atom in controlling silicide growth. The following planar composite systems were used for these studies.+

+The sputtering conditions may be found in Appendix A.

a. SiC (2.2 microns)/Ti used as a standard for all systems.

b. SiC (1.8 microns)/Al (0.800 microns)/Ti to study the rejection mechanism.

c. SiC (2.0 microns)/Mo_5Si_3 (1.0 micron)/Ti used to study the effectiveness of the barrier mechanism.

d. In addition to the above, samples of Mo_5Si_3 (1.8 microns)/Ti were used as standards for the SiC/Mo_5Si_3/Ti system.

e. SiC (2.2 microns)/Ti_3Al/Ti - to study the effectiveness of the two mechanisms with Ti_3Al acting as a barrier and with α-Ti (Al) retarding the reaction by rejection.

The substrates for all of the above composite systems were 7/8 inch in diameter and 0.11 inch thick discs. These were cut from a 99.5% purity alpha-Titanium sheet obtained from Semi-alloys Inc.[10]

Samples "a" through "d" were sputter-deposited by Perkin Elmer-Ultek, Inc.[11] Immediately before sputtering, the Ti wafers were sprayed with methol ethol ketone and dried with a blower.

The SiC films on the Ti_3Al substrates (e) were prepared at Virginia Tech. An attempt was made to duplicate the conditions used by Perkin Elmer for the SiC/Al/Ti system. However, due to differences in the base pressures used, it was necessary to obtain a new set of conditions to obtain the desired thickness (Table V-A). Prior to sputter deposition, the samples were thoroughly cleaned. The cleaning procedure included heating the samples in the following solvents:

Solvent	Max. Temp. (^oC)	Time of Immersion (min.)
Trichloroethylene	73	30
Acetone	56	30
Alcohol	65	30

After cleaning, the samples were thoroughly dried and carefully weighed using a Mettler[12] scientific balance accurate up to 10^{-6} gms. The surface was sprayed with dust-off[13] to remove dust particles before loading them into the specimen chamber of a Perkin Elmer 2400 RJ sputtering system. After sputtering for the desired length of time, the samples were weighed again. The film thickness was calculated from the difference in weight, density and specimen discussions.

INTERFACE REACTIONS IN PLANAR COMPOSITES

The various SiC/Ti planar composites with and without the protective coatings (Al and Mo_5Si_3) were characterized by X-ray diffraction in the as-received condition. In all the composites which had a SiC coating, the SiC was amorphous. The Mo_5Si_3 coatings in the as-sputtered condition were also amorphous while the Al and alpha-titanium were crystalline. From these initial diffraction patterns, there was no indication of any silicide formation during sputter-deposition and also no beta-titanium reflections were observed.

The SiC/Ti sample was investigated as a reaction rate standard. All samples were given a prior anneal for 2 hrs. at 600^oC before annealing at 875^oC for 1/2 hr., 1 hr., 2 hrs. and 4 hrs. During the degassing at 600^oC, there was no silicide formation.

X-ray diffraction was used to examine the reacted samples. After a 1/2 hour anneal at 875^oC, the SiC/Ti samples yielded significant

amounts of reaction products. Thirteen Ti_5Si_3 lines were identified. At this early stage, 5 lines from TiC and a couple of weak reflections from TiSi and $TiSi_2$ were observed. The SiC film did not stay completely intact even with slow furnace cooling after the 1/2 hr anneal. After annealing for longer times (1 hr., 2 hrs., 4 hrs.), it was observed that the film remained intact. A one-hour anneal at 875°C appears to represent a threshold for stabilizing the film against flaking.

X-ray studies on the samples annealed for 1 hr., 2 hrs., and 4 hrs., indicated that Ti_5Si_3 continued to form over the 4-hour period. After the 4-hour anneal, twenty-three Ti_5Si_3 lines were identified. The intensity of TiC, TiSi and $TiSi_2$ diffraction lines increased consistently from the half-hour to the 4 hour anneal. Of these compounds, the largest total intensity was from TiC and the smallest was from $TiSi_2$. The matrix gave 21 alpha titanium lines. The X-ray diffraction results on the SiC/Ti samples is presented in Table 1. The integrated intensity values were obtained by measuring peak areas above background, and the two-theta positions were corrected using a silicon powder standard (NBS #640). It should be noted that even after annealing 4 hrs. at 875°C the SiC phase did not crystallize.

When a SiC/Al/Ti sample was reacted at 875°C for 1/2 hour, some Ti_5Si_3 was formed. Although only 10 Ti_5Si_3 lines were identified, the integrated intensity from Ti_5Si_3 appeared to be comparable with that obtained from the SiC/Ti sample reacted for 1/2 hour. However, for longer reaction times, the amount of Ti_5Si_3 as well as the number of lines observed increased only slightly. No lines from TiSi and $TiSi_2$ were observed even up to the longest anneal (4 hours). During the early stages, no TiC reflections were noticed. However, after the 2 hour anneal, two TiC lines were identified. There was also some evidence of Ti_3AlC

TABLE 1

Integrated intensities and two theta positions for the SiC/Ti system annealed at 875°C for various times.

	1/2 hour		1 hour		2 hours		4 hours	
Identification	Int.	2θ	Int	2θ	Int	2θ	Int	2θ
Ti_5Si_3 (200)	6.0	27.648	11.9	27.658	33.5	27.658	35.1	27.671
Ti_5Si_3 (111)	6.3	29.361	12.1	29.558	10.8	29.558	11.1	29.571
TiSi (201)	-	-	4.2	31.808	6.1	31.883	3.5	31.838
TiSi (111)	-	-	-	-	9.8	33.132	7.2	33.132
Ti_5Si_3 (002)	14.6	34.723	19.3	34.732	4.9	34.745	7.3	34.770
α-Ti (100)	84.0	35.161	86.1	35.157	79.6	35.170	40.9	35.195
TiC (111)	74.9	36.021	87.7	36.027	115.2	36.045	147.7	36.070
TiSi (210)	22.5	36.348	30.3	36.532	25.4	36.632	22.6	36.620
Ti_5Si_3 (210)	30.9	36.873	35.3	36.882	100.4	36.870	108.9	36.895
Ti_5Si_3 (102)	40.9	37.461	52.5	37.587	13.9	37.507	14.8	37.507
TiSi (102)	-	-	-	-	37.6	37.695	47.5	37.695
α-Ti (002)	469.8	38.411	403.4	38.419	146.3	38.419	173.3	38.431
$TiSi_2$ (311)	13.3	39.598	27.9	39.754	26.8	39.869	34.3	39.831
α-Ti (101)	685.5	40.221	669.9	40.219	503.2	40.231	393.9	40.244
Ti_5Si_3 (211)	74.9	40.923	121.3	40.919	192.2	40.919	234.0	40.944
TiC (200)	99.9	41.836	151.6	41.831	139.4	41.844	165.4	41.869
{ Ti_5Si_3 (300) / $TiSi_2$ (004)	-	-	-	-	136.8	41.996	168.8	42.006
Ti_5Si_3 (112)	53.3	42.561	71.4	42.581	52.1	42.594	62.2	42.606
{ TiSi (301) / $TiSi_2$ (022)	5.5	43.473	8.9	43.684	11.2	43.781	9.8	43.769
TiSi (112)	7.2	45.361	14.3	45.58	16.5	45.718	17.8	45.694
TiSi (020)	-	-	-	-	5.1	51.055	6.7	51.068
Ti_5Si_3 (221)	-	-	2.5	52.204	7.4	52.217	8.2	52.230
α-Ti (102)	184.6	53.023	133.5	53.029	131.6	53.029	107.3	53.067
Ti_5Si_3 (311)	3.2	54.223	5.0	54.227	10.7	54.267	14.1	54.267
Ti_5Si_3 (400)	-	-	-	-	4.5	57.116	6.6	57.128
TiC (220)	25.7	60.611	40.8	60.604	68.1	60.666	77.9	60.690
Ti_5Si_3 (222)	10.2	61.348	14.3	61.350	17.9	6.1352	23.7	61.365
α-Ti (110)	81.1	63.011	61.7	63.027	60.5	63.040	63.5	63.077
TiSi (112,411)	-	-	-	-	3.2	65.190	5.9	65.177
Ti_5Si_3 (321)	5.4	65.685	6.6	65.690	15.4	65.590	16.2	65.627
Ti_5Si_3 (410)	14.8	66.438	21.4	66.427	28.1	66.427	21.1	66.415
Ti_5Si_3 (112)	-	-	-	-	-	-	15.4	66.588
Ti_5Si_3 (402)	5.7	68.547	8.1	68.602	9.9	68.577	14.2	68.590
α-Ti (103)	239.8	70.634	185.8	70.652	145.6	70.665	177.8	70.690
TiC (113)	10.4	72.559	21.7	72.552	28.3	72.627	38.9	72.640
Ti_5Si_3 (500,004)	-	-	6.8	73.502	4.2	73.390	9.9	73.402
$TiSi_2$ (602)	-	-	-	-	3.8	73.652	-	-
α-Ti (200)	9.5	74.259	8.9	74.227	4.8	74.252	5.3	74.265
α-Ti (112)	150.1	76.245	115.4	76.265	153.1	76.265	88.2	76.315

ORIGINAL PAGE IS
OF POOR QUALITY

Table 1 Continued

	1/2 hour		1 hour		2 hours		4 hours	
Identification	Int	2θ	Int	2θ	Int	2θ	Int	2θ
α-Ti (201)	75.9	77.408	59.2	77.427	69.3	77.440	72.1	77.477
Ti_5Si_3 (420)	-	-	-	-	4.9	78.405	10.4	78.427
Ti_5Si_3 (331)	-	-	1.8	79.381	6.8	79.352	9.0	79.365
α-Ti (004)	49.8	82.207	29.2	82.226	24.7	82.239	11.9	82.251
TiSi (114, 131)	-	-	-	-	2.7	83.351	3.0	83.414
Ti_5Si_3 (502)	4.0	83.750	6.2	83.801	13.3	83.751	12.3	83.763
Ti_5Si_3 (511)	-	-	1.2	86.001	4.6	86.001	6.3	85.938
α-Ti (202)	23.1	86.780	31.2	86.801	28.0	86.838	26.2	83.838
TiC (400)	2.3	91.125	2.6	91.050	4.7	91.122	8.2	91.060
α-Ti (104)	30.8	29.650	38.8	92.673	29.0	92.672	21.3	92.697
α-Ti (203)	66.9	102.336	76.6	102.370	82.7	102.395	84.9	102.433
TiC (420)	15.5	105.823	21.4	105.860	25.0	105.919	43.2	105.971
α-Ti (211)	55.9	109.085	66.5	109.138	56.0	109.169	52.5	109.207
α-Ti (114)	110.7	114.175	110.0	114.210	120.0	114.230	102.7	114.280
α-Ti (212)	43.4	119.250	30.0	119.325	34.0	119.340	16.2	119.415
α-Ti (105)	145.6	122.103	134.8	122.190	84.4	122.190	107.0	122.215
Ti_5Si_3 (532)	"	-	3.5	125.160	9.7	125.200	11.9	125.214
α-Ti (204)	28.4	126.250	25.2	126.310	23.1	126.327	13.6	126.377
{Ti_5Si_3 (206) / TiC (311)	-	-	-	-	5.7	136.100	14.6	136.100
α-Ti (213)	144.3	139.345	143.3	139.362	147.8	139.448	131.8	139.400
α-Ti (302)	138.2	148.470	87.0	148.480	128.7	148.635	70.2	148.698

ORIGINAL PAGE IS
OF POOR QUALITY

TABLE 2

Integrated intensities and two theta positions for the SiC/Al/Ti system annealed at 875°C for various times.

Identification	1/2 hour Int	1/2 hour 2θ	1 hour Int	1 hour 2θ	2 hours Int	2 hours 2θ	4 hours Int	4 hours 2θ
Ti_3Al (101)	33.4	26.196	41.5	26.196	49.0	26.171	44.0	26.096
Ti_5Si_3 (200)	7.8	27.646	6.7	27.571	6.6	27.521	6.1	27.608
Ti_3Al (110)	6.7	30.933	11.1	30.971	10.8	30.946	11.3	30.883
TiAl (110)	22.8	31.658	6.9	31.632	-	-	-	-
Ti_5Si_3 (002)	10.9	34.708	9.7	34.708	13.2	34.608	8.7	34.688
α-Ti (100)	49.6	35.171	38.1	35.157	28.1	35.157	29.4	35.195
Ti_3Al (200)	160.2	35.907	189.9	35.907	213.7	35.895	262.5	35.807
Ti_5Si_3 (210)	28.8	36.832	38.5	36.782	25.5	36.770	37.5	36.820
Ti_5Si_3 (102)	15.7	37.557	26.1	37.332	52.4	37.357	34.6	37.595
α-Ti (002)	152.1	38.470	132.6	38.457	116.8	38.495	187.0	38.500
Ti_3Al (002)	466.9	38.795	355.2	38.832	290.9	38.782	203.9	38.720
TiAl (111)	-	-	-	-	-	-	-	-
α-Ti (101)	312.6	40.232	302.8	40.231	207.8	40.244	238.0	40.256
Ti_3Al (201)	414.3	40.969	500.9	40.981	635.5	40.944	723.8	40.869
Ti_5Si_3 (300)	41.6	41.806	59.9	41.781	68.7	41.831	91.9	41.944
Ti_5Si_3 (112)	37.9	42.606	33.7	42.444	42.2	42.481	35.2	42.531
Ti_3AlC (200)	-	-	-	-	20.4	43.381	4.9	43.469
TiAl (002)	35.6	44.554	10.5	44.593	-	-	-	-
TiAl (200)	79.1	45.404	23.4	45.343	-	-	-	-
Ti_3Al (112)	5.6	50.494	8.1	50.505	8.3	50.417	6.1	50.317
Ti_2Al (201)	7.2	50.917	-	-	-	-	-	-
Ti_5Si_3 (221)	-	-	3.6	52.217	4.3	52.192	8.4	52.092
α-Ti (102)	84.9	53.043	80.2	53.044	66.8	53.053	55.5	53.041
Ti_3Al (202)	69.0	53.867	99.7	53.917	117.5	53.842	111.3	53.767
TiC (220)	16.6	60.534	16.7	60.528	23.4	60.330	37.8	60.850 }
Ti_5Si_3 (222)	7.3	61.378	5.7	61.378	7.8	61.264		
α-Ti (110)	61.5	63.015	43.8	63.016	55.7	63.027	46.7	63.040
Ti_3Al (220)	41.9	64.402	59.5	64.440	70.3	64.440	87.3	64.340
TiAl (202)	39.9	65.402	11.5	65.415	-	-	-	-
Ti_5Si_3 (410)	19.4	66.127	11.7	66.150	11.3	66.252	7.4	66.352
α-Ti (103)	149.4	70.077	144.7	70.692	124.2	70.690	120.5	70.677
Ti_3Al (203)	86.9	71.652	117.3	71.790	128.4	71.665	99.3	71.565
α-Ti (200)	-	-	-	-	-	-	6.1	74.277
Ti_3Al (400) } Ti_3AlC (311)	-	-	-	-	16.0	75.821	10.5	75.852
α-Ti (112)	110.0	76.272	74.2	76.265	68.8	76.290	66.1	76.277
α-Ti (201)	101.9	77.452 }	86.2	77.422	23.7	77.465	145.4	77.477 }
Ti_3Al (222)		77.752	116.7	77.817	117.7	77.790		77.715
Ti_3Al (401)	62.4	79.352	52.1	79.227	52.3	79.227	55.9	79.115
α-Ti (004)	41.0	82.277	22.8	82.314	21.0	82.314	27.7	82.314

ORIGINAL PAGE IS
OF POOR QUALITY

Table 2 Continued

	1/2 hour		1 hour		2 hours		4 hours	
Identification	Int	2θ	Int	2θ	Int	2θ	Int	2θ
Ti_3Al (004)	28.9	83.151	22.1	83.377	22.8	38.201	16.4	83.063
α-Ti (202)	14.2	86.825	11.9	86.828	10.6	86.825	20.1	86.838
Ti_3Al (402)	-	-	-	-	9.7	88.750	12.6	88.600
α-Ti (104)	29.7	92.722	25.5	92.759	26.5	92.772	20.8	92.736
Ti_3Al (204)	8.4	94.171	13.3	94.184	20.1	94.071	14.5	93.934
α-Ti (203)	41.8	102.405	20.4	102.420	56.1	102.420	56.1	102.408
Ti_3Al (403)	15.4	104.695	25.2	104.732	27.9	104.683	30.2	104.533
α-Ti (210)	8.4	105.919	6.6	105.932	7.0	105.932	9.6	105.908
α-Ti (211)	50.0	109.143	52.3	109.143	41.6	109.156	35.5	109.168
Ti_3Al (421)	31.9	112.268	36.4	112.380	39.9	112.393	49.5	112.206
α-Ti (114)	79.3	114.268	68.1	114.305	63.5	114.317	66.7	114.305
Ti_3Al (224)	20.4	116.672	33.1	116.780	47.2	116.730	39.0	116.517
α-Ti (212)	22.9	119.342	17.4	119.355	11.8	119.366	15.7	119.329
α-Ti (105)	77.1	122.291	81.3	122.315	84.6	122.328	106.2	122.290
Ti_3Al (205)	14.2	124.450	30.0	124.615	42.2	124.514	28.6	124.327
α-Ti (204)	18.3	126.240	18.6	126.377	17.4	126.402	10.2	126.414
αTic (422)	18.4	129.340	16.4	129.602	18.9	129.638	16.7	129.676
α-Ti (213)	114.7	139.413	89.6	139.498	73.6	139.523	61.8	139.560
Ti_3Al (423)	26.9	145.050	-	-	64.4	145.210	71.6	144.963
α-Ti (302)	59.9	148.660	86.9	148.350	51.2	148.635	55.2	148.660

ORIGINAL PAGE IS
OF POOR QUALITY

TABLE 3

Integrated intensities and two-theta positions for the $SiC/Mo_5Si_3/Ti$ planar composites

$SiC/Mo_5Si_3/Ti$	1/2 hour		1 hour		2 hours		4 hours	
Identification	Int	2θ	Int	2θ	Int	2θ	Int	2θ
Ti_5Si_3 (200)	11.49	27.670	11.89	27.713	21.95	27.658	28.97	27.671
Ti_5Si_3 (111)	15.07	29.633	15.90	29.646	19.85	29.583	18.14	29.583
Ti_5Si_3 (002)	59.52	34.858	50.95	34.871	59.59	34.796	54.61	34.796
TiC (111)	-	-	32.85	36.058	134.35	36.046	148.11	36.083
Mo_5Si_3 (002)	16.89	36.607	-	-	-	-	-	-
Ti_5Si_3 (210)	47.01	36.919	39.03	36.957	75.58	36.899	74.99	36.895
Ti_5Si_3 (102)	65.45	37.644	56.96	37.645	84.70	37.595	70.79	37.595
α-Ti (002)	39.05	38.544	21.84	38.570	-	-	-	-
β-Ti (110)	387.69	39.132	292.43	39.132	893.11	39.132	750.64	39.170
Mo_5Si_3 (330)	903.73	39.532	887.07	39.382	4.62	39.782	-	-
α-Ti (101)	281.68	40.168	40.83	40.256	16.43	40.181	20.07	40.094
Ti_5Si_3 (211)	147.19	40.981	144.23	41.019	212.23	40.964	229.68	40.970
Ti_5Si_3 (300)	24.44	42.056	53.45	42.056	115.22	42.006	125.08	42.019
Ti_5Si_3 (112)	243.59	42.706	198.66	42.719	236.48	42.656	231.64	42.681
Ti_5Si_3 (202)	13.13	45.105	9.16	45.080	8.98	44.994	9.87	45.030
Mo_5Si_3 (222)	17.90	45.430	3.21	45.480	-	-	-	-
Ti_5Si_3 (221)	-	-	-	-	5.26	52.243	7.24	52.293
α-Ti (102)	27.65	53.054	10.39	53.092	9.65	53.092	4.89	52.779
Ti_5Si_3 (311)	2.90	54.328	4.11	54.341	15.37	54.304	13.33	54.292
β-Ti (200)	23.33	56.503	31.24	56.511	223.92	56.515	219.26	56.578
Ti_5Si_3 (400)	257.12	57.09	259.19	56.891	-	-	-	-
TiC (220)	-	-	11.09	60.702	42.41	60.664	58.52	60.740
Ti_5Si_3 (222)	9.70	61.515	33.34	61.502	39.49	61.402	40.57	61.427
α-Ti (110)	9.03	63.015	4.83	63.066	-	-	-	-
Ti_5Si_3 (312)	11.76	63.278	4.74	63.415	14.68	63.302	7.88	63.277
Ti_5Si_3 (321)	6.82	65.727	7.72	65.765	14.13	65.665	16.62	65.665
Ti_5Si_3 (213)	22.28	66.739	46.94}	66.653}	63.09	66.565	61.70	66.566
Mo_5Si_3 (442)	19.11	66.632			-	-	-	-
Ti_5Si_3 (402)	13.12	68.779	15.17	68.752	20.15	68.653	23.86	68.663
β-Ti (211)} α-Ti (103)	140.99	70.814	105.11	70.863	236.48	70.877	200.80	70.940
TiC (113)	-	-	-	-	13.82	72.627	18.04	72.777
Ti_5Si_3 (004, 500)	53.59	73.538	37.16	73.539	25.96	73.512	26.82	73.502
α-Ti (112)	32.10	76.327	17.31	76.377	-	-	-	-
TiC (222)	-	-	-	-	28.83	76.412	13.44	76.490
α-Ti (201)	25.63	77.427	16.39	77.365	23.68	77.277	9.86	77.115
Ti_5Si_3 (420)	-	-	-	-	8.34	78.502	3.77	78.502
Ti_5Si_3 (331)	-	-	-	-	5.24	79.427	4.44	79.465

ORIGINAL PAGE IS
OF POOR QUALITY

ORIGINAL PAGE IS OF POOR QUALITY

Table 3 Continued

SiC/Mo_5Si_3.Ti	1/2 hours		1 hour		2 hours		4 hours	
Identification	Int	2θ	Int	2θ	Int	2θ	Int	2θ
α-Ti (004)	11.02	82.501	7.39	82.439	-	-	-	-
Ti_5Si_3 (502)	34.82	84.076	51.07	84.062	75.87	84.051	82.39	84.026
Ti_5Si_3 (214)	58.83	85.188	31.25	85.133	10.65	85.126	10.83	85.189
Ti_5Si_3 (511)	-	-	-	-	4.01	86.026	4.92	86.064
α-Ti (202) Mo_5Si_3 (750)	17.85	87.038	13.93	87.000	19.07	87.050	19.92	87.038
Ti_5Si_3 (304)	10.59	88.505	12.14	88.525	16.80	88.462	19.80	88.475
α-Ti (104)	16.60	92.822	-	-	--	-	-	-
Mo_5Si_3 (514, 662)	23.93	96.996	27.36	96.960	75.14	96.922	75.95	96.922
Mo_5Si_3 (930)	87.90	98.171	68.98	97.696	-	-	-	-
Mo_5Si_3 (851)	4.36	100.033	-	-	-	-	-	-
α-Ti (203)	23.16	102.270	19.20	102.408	20.47	102.333	18.48	102.000
TiC (420)	-	-	-	-	4.74	105.920	13.86	105.120
Ti_5Si_3 (215)	9.55	108.619	20.18	108.970	24.51	108.594	23.39	108.632
β-Ti (222)	-	-	-	-	21.37	110.206	14.90	110.382
α-Ti (114)	18.02	114.567	13.45	114.604	22.67	114.506	-	-
α-Ti (212)	6.90	119.290	6.30	119.490	3.00	119.140	-	-
Ti_5Si_3 (621)	15.40	122.040	12.36	122.030	25.06	121.940	13.71	121.960
α-Ti (105)	26.40	122.565	28.52	122.565	-	-	-	-

being formed, although overlapping lines prevented an unambiguous identification. Only one separated high angle line was found, and this remained constant up to the 4 hour anneal. If this is due to Ti_3 AlC, the amount of this phase remains constant.

For the shorter times (1/2 hour and 1 hour), 6 lines from the tetragonal TiAl phase (a = 4.015A, c = 4.062A) were observed. These lines decreased in intensity consistently from the 1/2 hour to the 1 hour anneal and disappeared after 2 hours. Also, the lattice tended to become more and more cubic before the TiAl lines disappeared.

Starting from 1/2 hour and up to 4 hours, a number of diffraction peaks from Ti_3Al phase were identified. The amount of Ti_3Al increased systematically from 1/2 hour to 4 hours and 20 lines were observed. The lines from the matrix were entirely from the alpha-phase as expected since Al would tend to stabilize this phase. As noted in the SiC/Ti system, the SiC phase did not crystallize upon annealing. The integrated intensities as well as two-theta positions for the various phases are presented in Table 2.

The Mo_5Si_3/Ti system was used for a comparison with the SiC/Mo_5Si_3/Ti planar composites. These samples were reacted at 875°C for 1/2 hr., 1 hr., 2 hrs. and 4 hours. X-ray diffraction analysis revealed at least 25 lines from the Ti_5Si_3 phase. This would appear surprising at first, since one would expect that without a SiC coating, no silicide should form. The diffraction pattern after the 1/2 hour anneal on this sample revealed a number of lines from Mo_5Si_3 and a few from Mo_3Si although the Mo_5Si_3 layer appeared to be amorphous in the as-sputtered state. The presence of Mo_3Si is supported by a recent M.S. thesis[14] which was concerned with studies on Mo_5Si_3 thin films on Si single crystal substrates. It appears that when Mo_3Si is located at the titanium interface, it dissociates according to:

ORIGINAL PAGE
BLACK AND WHITE PHOTOGRAPH

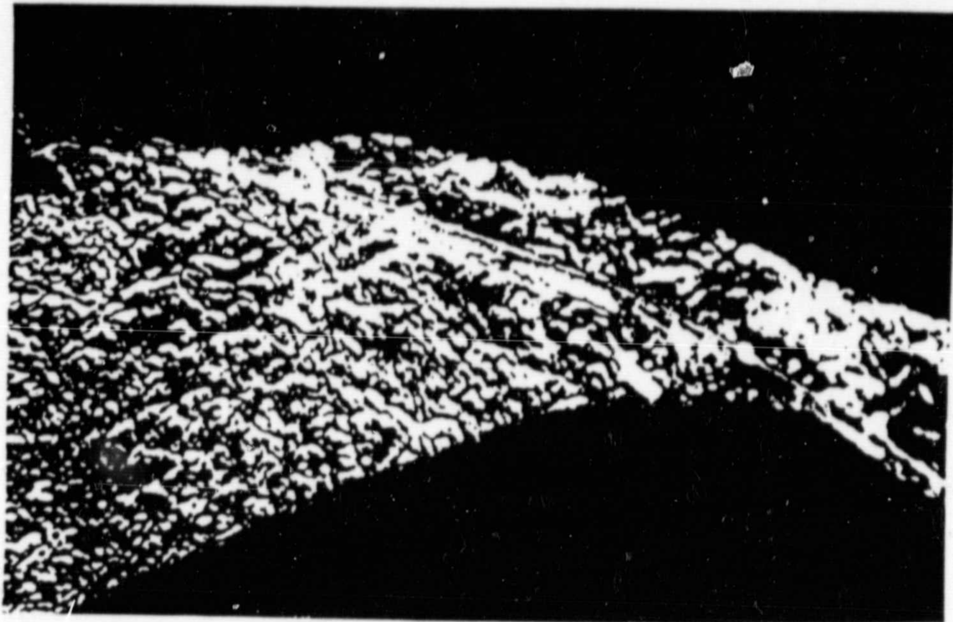

Magfn. 630X

Fig. 1 Photomicrograph of the SiC/Ti sample reacted at 875°C for 1/2 hr. (polarized light).

ORIGINAL PAGE
BLACK AND WHITE PHOTOGRAPH

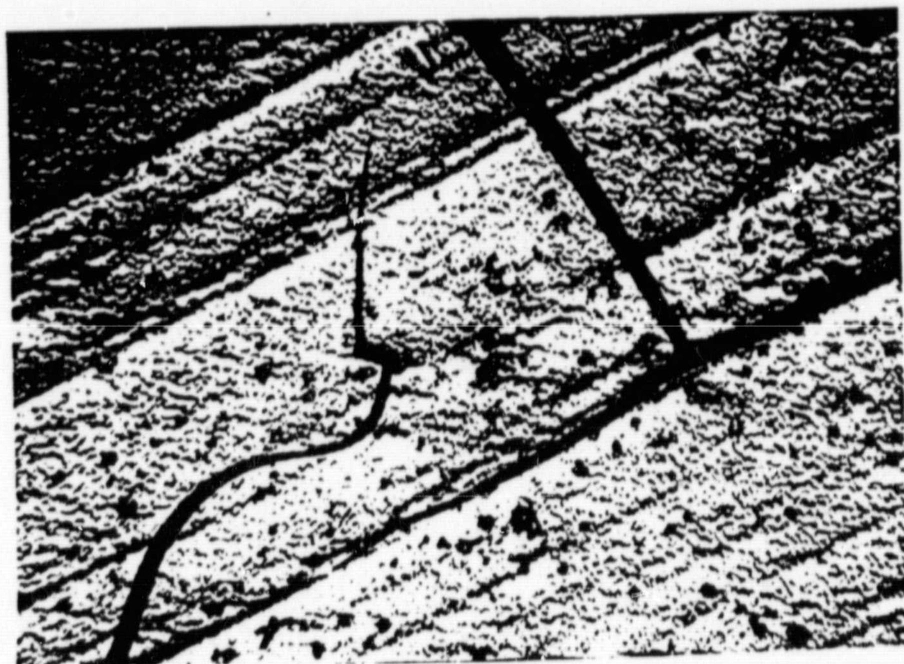

Magfn. 630X

Fig. 2 Photomicrograph of the SiC/Al/Ti sample reacted at 875°C for 1/2 hr., showing discontinuous reaction zones.

ORIGINAL PAGE
BLACK AND WHITE PHOTOGRAPH

ORIGINAL PAGE
BLACK AND WHITE PHOTOGRAPH

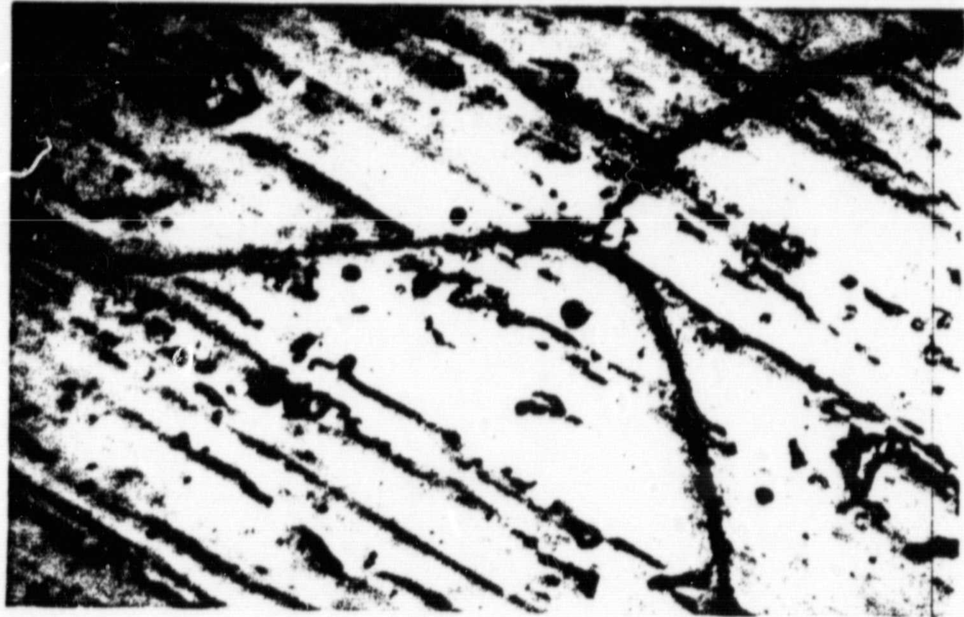

Magfn. 630X

Fig. 3 Photomicrograph of the $SiC/Mo_5Si_3/Ti$ sample reacted at 875^oC for 1/2 hour.

ORIGINAL PAGE
BLACK AND WHITE PHOTOGRAPH

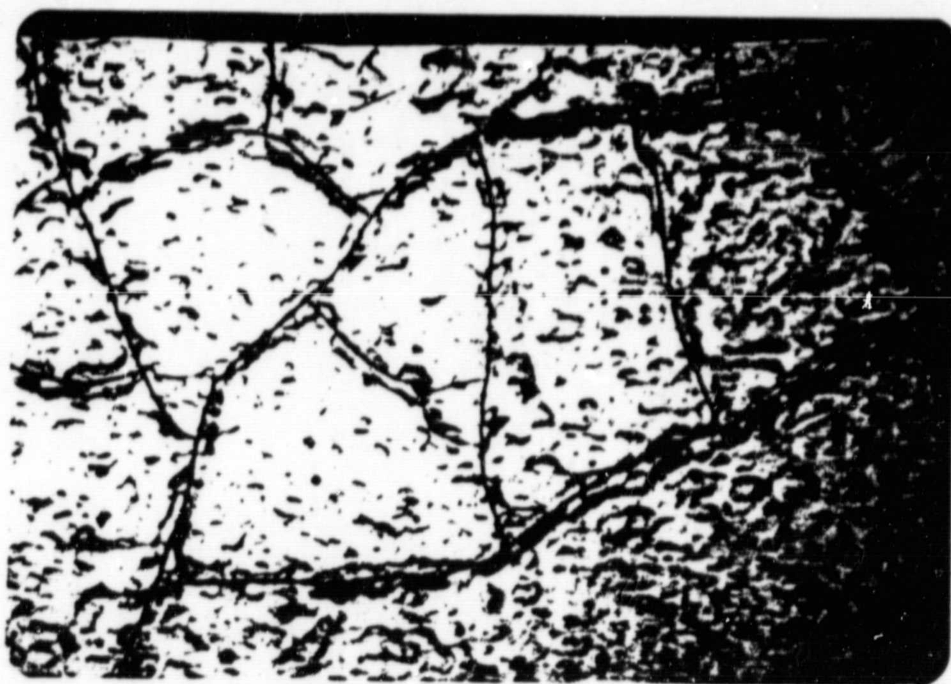

Magfn. 40X

Fig. 4 Photomicrograph of the SiC/Ti sample reacted at 875°C for 2 hours.

ORIGINAL PAGE
BLACK AND WHITE PHOTOGRAPH

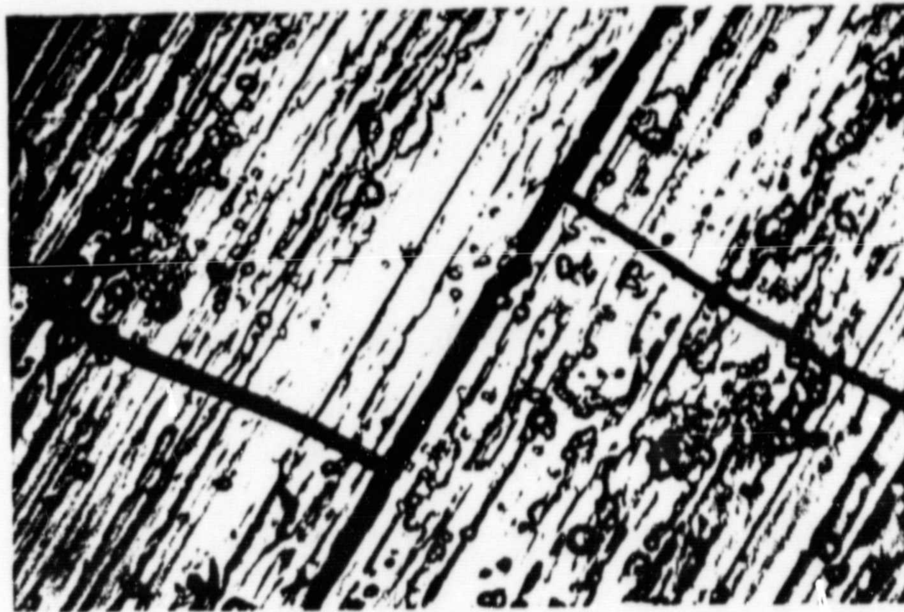

Magfn. 630X

Fig. 5 Photomicrograph of the SiC/Al/Ti sample reacted at 875°C for 2 hours.

ORIGINAL PAGE
BLACK AND WHITE PHOTOGRAPH

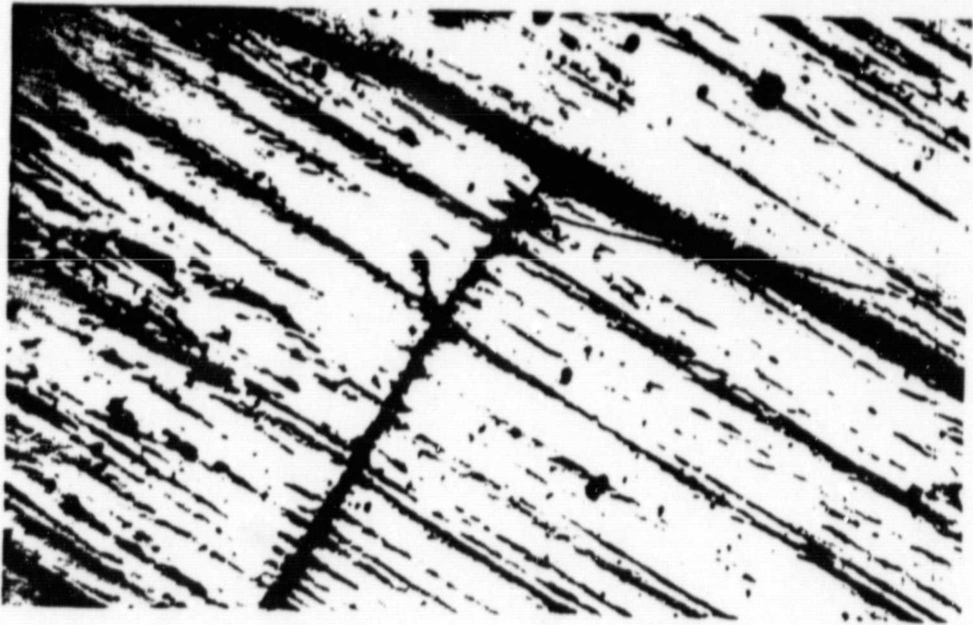

Magfn. 630X

Fig. 6 Photomicrograph of the $SiC/Mo_5Si_3/Ti$ sample reacted at 875^oC for 2 hours.

$$Mo_3Si \longrightarrow 3\ Mo + Si$$

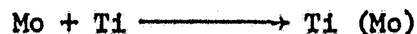

$$Mo + Ti \longrightarrow Ti\ (Mo)$$

Free Si forms Ti_5Si_3 in the crystalline state. This observation is consistent with a decrease in the intensity of the Mo_3Si diffraction lines for longer annealing times and the formation of the β-titanium phase at the expense of α-titanium. In other words, the solution of Mo in titanium serves to stabilize the β-phase.

Optical Microscopy - Unetched samples were examined under a Reichert microscope using polarized light and an oblique illuminator. The SiC/Ti samples showed a reaction zone, even after only 1/2 hr. Figure 1 shows the surface of a SiC/Ti sample with a reaction zone along the Ti grain boundaries and the rough underlying Ti surface which also appears to have reacted before flaking. The roughness pattern is not characteristic of the unreacted Ti surface. The width of the reaction zone increases with increasing reaction times and this seems to correlate well with the increase in the amount of reaction products as observed by x-ray diffraction.

Figures 2 and 3 show the photomicrographs for SiC/Al/Ti and $SiC/Mo_5Si_3/Ti$ reacted for 1/2 hr. at 875°C. In these cases, there are large regions of discontinuous boundary zones, however the widths of these grain boundary zones are smaller than for SiC/Ti samples.

Figures 4, 5, and 6 illustrate that annealing for 2 hrs. at 875°C greatly reduces the tendency for flaking and crack formation in all three samples. The grain boundary reaction within SiC/Al/Ti and $SiC/Mo_5Si_3/Ti$ samples has continued and no longer appears to be discontinuous. Unfortunately, the planar interface reaction with Ti is not observable in these photomicrographs.

RELATIVE REACTION RATES

Several x-ray methods were examined in order to arrive at a quantitative method that inter-relates the rate of silicide formation. The most obvious method would have been to follow the rate of decrease of SiC. However, the lack of crystalline reflections from SiC made this task impossible since changes in the amorphous scattering from SiC did not give meaningful results. However, one method gave systematic results that was found useful for evaluating the effectiveness of Mo_5Si_3 and Al films.

The major silicide product associated with SiC/Ti matrix reactions has been Ti_5Si_3. This phase also gives a large number of diffraction lines in this investigation. In previous studies,[15] one finds that the initial stage of interface reaction is important in determining the mechanical properties of composites. Ideally, one would like to obtain as-pressed composites in the earliest stage of this interface reaction. If one concentrates on this stage, it is possible to make certain simplifying assumptions that enable x-ray data to be interpreted without a detailed model of the morphology of the various reaction products. It is assumed that the rate limiting step for the reaction is the diffusion of Si from the SiC filament to the titanium substrate and that we are dealing with a very thin layer of reaction product that is mainly Ti_5Si_3. With a very tin layer of reaction product, the absorption of the incident and diffracted beams for both Ti_5Si_3 and titanium diffraction lines is nearly the same.

Ten pairs of Ti_5Si_3 alpha-titanium lines were selected such that each pair had nearly the same Bragg angles. Pairing in terms of Bragg angle

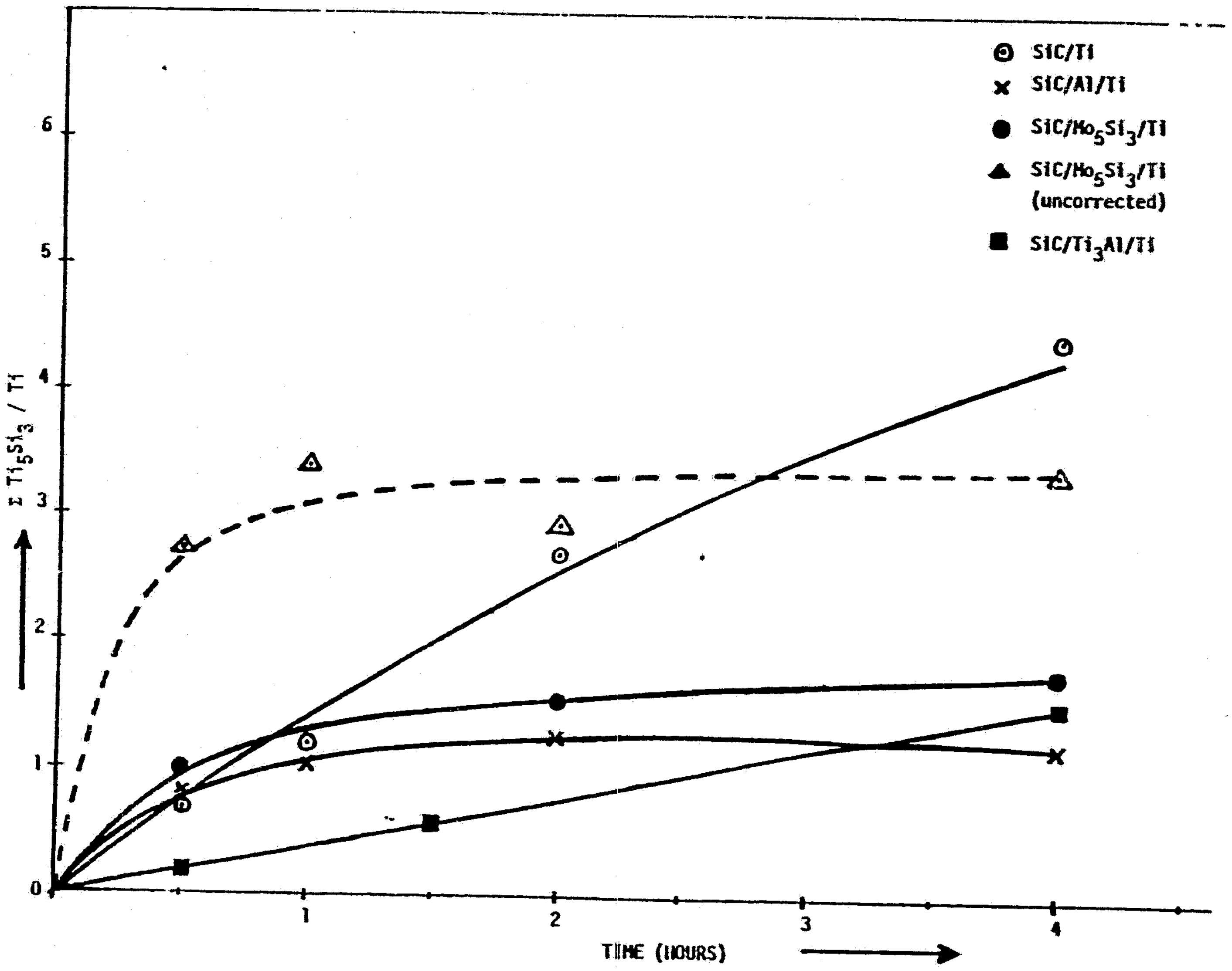

Figure 7: Reaction rate curves for the various planar composite systems.

gives nearly equivalent absorption path lengths. By summing all ten ratios, a set of internally consistent plots are obtained for all annealed samples.

The Mo_5Si_3 barrier film presented special problems because the dominant substrate phase was beta-titanium and not alpha-titanium. To overcome this difficulty, the total beta integrated intensity was redistributed into the ten alpha-titanium lines according to the theoretical distribution as obtained from the integrated intensity for random powders. It was found that Mo_5Si_3/Ti samples also give the Ti_5Si_3 phase and a beta-titanium matrix. In fact, this amount of Ti_5Si_3 accounts for about 50% of the Ti_5Si_3 intensity from SiC/Mo_5Si_3/Ti samples. In order to relate all results to Ti_5Si_3 formation which is associated with Si originating from the SiC, a correction was necessary for the SiC/Mo_5Si_3/Ti samples. The intensity for each Ti_5Si_3 line from a Mo_5Si_3/Ti sample was corrected to that associated with the SiC/Mo_5Si_3/Ti sample and subtracted. The intensity ratios were then formed and summed over pairs (see solid curve in Fig. 7). The dashed curve illustrates the uncorrected results for SiC/Mo_5Si_3/Ti samples.

The data for SiC/Ti samples that flaked after a half-hour reaction also had to be corrected. This was made using the area fraction of flaked film. The titanium intensities were decreased in proportion to the amount of absorption that would have resulted if the SiC film remained intact. Likewise, the Ti_5Si_3 intensities were increased and this calculation was based on the area fraction lost as a result of flaking as well as, the absorption within the SiC overlayer.

Figure 7 shows the sum of the integrated intensity ratios from Ti_5Si_3 and alpha-titanium increases continuously with reaction time for SiC/Ti samples. This curve is compared with those for the SiC/Al/Ti and

$SiC/Mo_5Si_3/Ti$ samples to determine the effectiveness of a coating in retarding silicide formation.

Beyond 1-hour both Mo_5Si_3 and Al reduce the rate at which Ti_5Si_3 forms from those silicon atoms originating from the SiC coating. These results also indicate that there is little difference between the three samples up to one-hour.

It must be emphasized that it is not known whether the formation of Ti_5Si_3 from the reaction of Mo_3Si with Ti will degrade the mechanical properties. The results from optical microscopy suggests that it might not since these films are less likely to flake than the SiC/Ti samples. An additional complication with this sample arises from the release of molybdenum into the titanium substrate and the related formation of the β-phase. Molybdenum, of course, is a β-stabilizer.

The curve for SiC/Al/Ti in Fig. 7 shows a trend similar to the $SiC/Mo_5Si_3/Ti$ composites. During the first hour at 875°C, it is evident that the Al film is not very effective in reducing silicide formation. This is due to the presence of Al-Ti compounds that prevent the release of Al into the titanium matrix. Data for samples annealed at 600°C for 2-hours shows that there is a small amount of Al solid solubility. This remains nearly constant up to 1 hour at 875°C. During this period, Ti-Al compounds continue to form and dissolve. For longer times, the only Ti-Al compound is Ti_3Al. When this dissolves, Al is released to the solid solution. This gives a reduced reaction rate because of Al rejection.

A detailed study of the release of Al into α-titanium from the decomposition of Ti_3Al is given in the next secion. For the present, one can determine the influence of this release on the reaction rate

by examining a set of samples containing SiC/Ti_3Al/Ti. These results are also given in Fig. 7. It would appear that a thin layer of Ti_3Al ($\approx$ 1.5 microns) is capable of providing immediate protection during the critial hot-pressing stage.

REFERENCES

1. "High Temperature Ti Composites," Air Force Materials Lab., Wright Patterson Air Force Base, Ohio, AFML-TR-73-223, Sept., 1973.

2. Metcalfe, A. G., "Interfaces in Metal Matrix Composites," (Academic Press, N.Y., 1974).

3. Schmitz, G. K., and Metcalfe, A. G., "Development of Continuous Filament Reinforced Metal Tape," AFML-TR-68-41, Feb. 1968.

4. Ratliff, J. C., and Powell, G. W., "Research on Diffusion Multiphase Systems, Reaction Diffusion in Ti/SiC and Ti-6Al-4V/SiC Systems," AFML-TR-70-42, Mar. 1970.

5. Snide, J. A., "Compatibility of Vapor Deposited B, SiC, and TiB_2 Filaments with Several Ti Matrices," AFML-TR-67-354, Feb., 1968.

6. Orszagh, J. and van der Poorten, H., Rev. Int. Hautes Temper. et Refract., Vol. 11 (2), 1974, p. 109-112.

7. Fitzer, E., and Schmidt, F. K., High-Temp.-High Press., Vol. 3, No. 4, 1971, p. 445-460. In German.

8. Schob, O., Nowotny, H. and Benesovsky, F., "The Ternary System (Ti, Zr, Hf)-Al-Si," Planseeber., Pulvermetall, Vol. 10, 1962, p. 65-71.

9. Pailler, R., Lahaye, M., Thebault, J., and Naslain, R., "Chemical Interaction Phenomena at High Temperature Between Boron Fibers and Ti Metal (or TA6V alloy)," Fall Meeting of TMS-AIME, Chicago, Oct. 1977.

10. Semi-alloys Inc., 888 S. Columbus Ave., Mount Vernon, New York 10550.

11. Perkin Elmer Ultek Inc., P.O. Box 10920, Palo Alto, California 94303.

12. Mettler Instr. Corp., Hightstown, N.J.

13. Dustoff, Manostat, 519, 8th Ave., N.Y., N.Y. 10018.

14. Smith, T. M., Masters Thesis, VPI & SU, Aug. 1980.

15. Rao, V. B., Houska, C. R., Unnam, J., Brewer, W. D., and Tenney, D. R., "Interfacial Reactions in Borsic/Ti-3Al-2.5V Composites," Proceedings of the TMS-AIME Fall Meeting, Oct., 1978.

APPENDIX A - SPUTTER DEPOSITION CONDITIONS

TABLE I-A

Specimen Data Sheet for SiC/Ti Planar Composites

Conditions		
Thickness Required	20,000 (SiC)	Å
Initial Press.	$2.8\text{X}10^{-7}$	Torr
Argon Press.	10	m Torr
Sputter Etch		
Time	30	min.
Substrate Bias	375	volts
Forward Power	1000	watts
Reflected Power	5-10	watts
Deposition		
Mode	RF Diode-Static	
Time	200	min.
Target Bias	1900	volts
Substrate Bias	0	volts
Forward Power	500	watts
Reflected Power	15-20	watts
Anode Spacing	2.5	inches
Deposition Rate	217.5	Å/1kw-min.
Substrate Temp.	250-300	°C
Actual Thickness	21,750	Å (± 10%)

TABLE II-A

Specimen Data Sheet for SiC/Al/Ti Planar Composites

Parameter	Value	Unit
Conditions		
First Thickness Req.	10,000 (Al)	Å
Second Thickness Req.	20,000 (SiC)	Å
Initial Press.	6.5×10^{-7}	Torr
Argon Press.	10	m Torr
Sputter Etch		
Time	30	min.
Substrate Bias	290	volts
Forward Power	1000	watts
Reflected Power	5-10	watts
Sputter Deposition Al (8" Target)		
Mode	D.C. Magnetron-Rotation	
Time	21	min.
Target Bias	360	volts
Substrate Bias	0	volts
Forward Power	3816	watts
Reflected Power	0	watts
Anode Spacing	2.5	inches
Deposition Rate	100.2	A/1kw-min.
Substrate Temp.	< 200	°C
Actual Thickness	8,000	Å (± 10%)
Sputter Deposition SiC (6" Target)		
Mode	RF Diode Static	
Time	200	min.
Target Bias	1750	volts
Substrate Bias	0	watts
Forward Power	500	watts
Reflected Power	5	watts
Anode Spacing	2.5	inches
Deposition Rate	217.5	Å/1kw-min.
Substrate Temp.	250-300	°C
Actual Thickness	18,250	Å (± 10%)

TABLE III-A

Specimen Data Sheet for the SiC/Mo_5Si_3/Ti Planar Composites

Conditions

First Thickness Req.	10,000 (Mo_5Si_3)	Å
Second Thickness Req.	20,000 (SiC)	Å
Initial Press.	$3.7X10^{-7}$	Å
Argon Press.	10	m Torr

Sputter Etch

Time	30	min.
Substrate Bias	0	volts
Forward Power	1000	watts
Reflected Power	10	watts

Sputter Deposition Mo_5Si_3 (6" Target)

Mode	RF Diode-Static	
Time	40.7	min.
Target Bias	1800	volts
Substrate Bias	0	volts
Forward Power	500	watts
Reflected Power	5	watts
Anode Spacing	2.5	inches
Deposition Rate	491.1	A/1kw/min.
Substrate Temp.	250-300	°C
Actual Thickness	10,000	Å (± 10%)

Sputter Deposition SiC (6" Target)

Mode	RF Diode-Static	
Time	183.9	min.
Target Bias	1750	volts
Substrate Bias	0	volts
Forward Power	500	watts
Reflected Power	5	watts
Anode Spacing	2.5	inches
Depositon Rate	217.5	Å/1kw/min.
Substrate Temp.	250-300	°C
Actual Thickness	20,000	Å (± 10%)

TABLE IV-A

Specimen Data Sheet for Mo_5Si_3/Ti Planar Composites

Conditions		
Thickness Req.	20,000	Å
Initial Press.	2.8×10^{-7}	Torr
Argon Press	10	m Torr
Sputter Etch		
Time	30	min.
Substrate Bias	340	volts
Forward Power	1000	watts
Reflected Power	20-25	watts
Sputter Deposition		
Mode	RF Diode-Static	
Time	73.8	min.
Target Bias	1700	volts
Substrate Bias	0	volts
Forward Power	500	watts
Reflected Power	5	watts
Anode Spacing	2.5	inches
Deposition Rate	491.1	Å/1kw/min.
Substrate Temp.	250-300	°C
Actual Thickness	18,125	Å (± 10%)

TABLE V-A

Specimen Data Sheet for Al/Ti Planar Composites

	1 micron	0.5 micron	
Conditions			
Thickness Requried	10,000	5000	Å
Initial Press	$3X10^{-7}$	$1.5X10^{-6}$	Torr
Ar Press	7	10	m Torr
Sputter Etch			
Time	5	5	min.
Substrate Bias	Unkonwn	1800	volts
Forward Power	1000	1000	watts
Reflected Power	5	approx. 0	watts
Deposition			
Mode	RF Diode - Static		
Time	21.3	12.68	min.
Target Bias	1700	1900	volts
Substrate Bias	0	0	volts
Forward Power	1000	1000	watts
Reflected Power	5	approx. 0	watts
Anode Spacing	1.5		
Deposition Rate	470	-	Å/1kw-min.
Substrate Temp.	254 to 300	Not Known	°C
Actual Thickness	10,000	4,800	Å (± 10%)

REACTIONS AND DIFFUSION BETWEEN AN Aℓ FILM AND A Ti SBUSTRATE

V. B. Rao and C. R. Houska

ABSTRACT

The reaction between a 0.5-1.0 micron Aℓ film and a thick Ti substrate to form Ti $A\ell_3$ occurs very rapidly on heating to 635°C and causes the Aℓ to be confined to the surface region. After heating to 900°C Ti_3 Aℓ is formed with little release of Aℓ into α-Ti. Further annealing at 900°C eventually causes the Ti_3 Aℓ phase to decompose and a substantial amount of Aℓ is released into α-Ti. The interdiffusion diffusion coefficient for Aℓ in α-Ti at 900°C was found to increase by less than one order of magnitude as Aℓ is varied from 0 to 20 at. %. These data were obtained from the (101) x-ray diffraction intensity band using polycrystalline samples. Improvements in the analysis of x-ray diffraction data for the determination of composition profiles are discussed.

V. B. Rao is a Materials Scientist III at Tektronix, Beaverton, Oregon 97077, and C. R. Houska is Professor of Materials Engineering, Virginia Polytechnic Institute and State University, Blacksburg, Virginia 24061

INTRODUCTION

When composites containing SiC fibers and a Ti matrix are reacted at elevated temperatures, brittle silicides are formed at the fiber-matrix interface. Normally, this is accompanied by a sizeable decrease in specific volume. The formation of brittle silicides and possible microcracks resulting from volume changes leads to a deterioration of the mechanical properties of SiC/Ti matrix composites.[1] This problem has prompted investigations with various intermediate coating materials that retard the silicide reaction. The use of Aℓ coatings or films prior to hot pressing has resulted in composites with improved mechanical properties. Optimum composites appear to be prepared from a two-step reaction carried out prior to hot pressing. At this stage, only Ti_3 Aℓ and α-Ti are present in the foils with Ti_3 Aℓ releasing Aℓ into α-Ti as it decomposes at hot pressing temperatures. The release of Aℓ into α-Ti close to the SiC/α-Ti interface provides control over interface reactions.

This paper deals with the formation of intermetallic compounds in the Ti-Aℓ system, particularly the early stages of Ti_3 Aℓ decomposition which provides the first large scale release of Aℓ into α-Ti. The small dimensions of these intermetallic compound films and the diffusion zone make x-ray diffraction an especially suitable technique[2] for these studies. Because prior x-ray investigations of this type have used single crystals and this study involves a polycrystalline substrate, some modifications in the theory are required. Other improvements are discussed that reduce the overall time and effort required to reduce the x-ray data to composition profiles.

THEORY

The diffracted x-ray intensity expression is based upon a diffused polycrystalline sample with a constant correction for texture. Although a polycrystalline sample gives much weaker diffraction patterns than a single crystal, useful results can often be obtained.

It has been customary to assume that all line broadening is given by a Cauchy or a Gaussian function. During the early stage of diffusion a Cauchy form best describes the line broadening; however, after prolonged diffusion the shape becomes Gaussian.[3] Neither a Gaussian or Cauchy function gives a really good fit during the transition. This difficulty is eliminated by using the Pearson VII distribution (hereafter P-VII) which contains an additional parameter "m" that takes the function smoothly from a Cauchy (m = 1), to a modified Lorentzian (m = 2) or a Gaussian ($m \geq 20$). This function provides a good fit between the computer simulated intensity bands and the data. It can fit most symmetrical diffraction peaks using only four parameters.[4] A fifth is required if the broadening from samples of homogeneous composition is asymmetric.

The lattice parameter or composition profile is assumed to be one-dimensional and is refined by a trial and error iterative process until the computer simulated intensity band agrees with the data.[2,3] This procedure is normally carried out on a graphics computer terminal. It was found that a function consisting of a sum of two or three error functions gives equally good results and is much less tedius to work with than adjusting an entire set of points that define the composition profile.

These three modifications i.e. using polycrystalline materials, the P-VII, and the analytical form for the composition profile are described

by the equations that follow. The kinematic integrated intensity is written in the usual way in terms of effective volume V^g_{je} for material of composition "j"[2]

$$P_j = I_o Q_j V^g_{je} \tag{1}$$

where I_o is the intensity of the incident beam and Q_j for a homogeneous polycrystalline material is defined by[5]

$$Q_j = \text{const.} \frac{\lambda^3}{v_j^2} \left[\frac{1 + \cos^2 2\theta_j \cos^2 2\theta'}{(1 + \cos^2 2\theta') \sin \theta_j \sin 2\theta_j} \right] p F^2_{j,T} \tag{2}$$

with $2\theta_m$ and $2\theta'$ representing the angles between incident and diffracted beams for element "j" in the sample and the monochromator. Also, λ, v_j, $F_{j,T}$, and p are the wavelength, unit cell volume, structure factor and multiplicity. Three expressions for the effective volume are required for this study.[2] The first represents the effective volume for a finite homogeneous film of thickness, ΔY_f

$$V^g_{fe} = g_f \frac{A_o}{2\mu_f} \left\{ 1 - \exp\left(- \frac{2\mu_f \, \Delta Y_f}{\sin\theta_f} \right) \right\}, \tag{3}$$

where A_o is the cross sectional area of the incident beam, g_f and μ_f are the orientation factor and linear absorption coefficient for a homogeneous film. The effective volume for a thick substrate containing a homogeneous film as an overlayer is

$$V^g_{se} = g_s \frac{A_o}{2\mu_s} \exp\left(- \frac{2\mu_f \, \Delta Y_f}{\sin\theta_s} \right), \tag{4}$$

where g_s and μ_s are the orientation factor and linear absorption coefficient for a homogeneous substrate. And, the effective volume for composition "j" in a substrate with a one-dimensional composition variation is given by

$$\Delta V^g_{je} = g_s \frac{A_o}{2\mu_j} \left[\exp \left(- \frac{2 \langle \mu(Y) \rangle_j (Y_j - \frac{1}{2}\Delta Y_j)}{\sin\theta_j} \right) \right] \left[1 - \exp \left(- \frac{2\mu_j \ \Delta Y_j}{\sin\theta_j} \right) \right] \tag{5}$$

where $\langle \mu(Y) \rangle_j$ is the average linear absorption coefficient between the upper boundary of element "j" and the free surface, μ_j and ΔY_j are the linear absorption coefficient for a homogeneous element and its thickness. In this approximation, a continuous composition variation is approximated by a series of small elements at constant composition located at $Y_j - \frac{1}{2} \Delta Y_j < Y_j < Y_j + \frac{1}{2} \Delta Y_j$ relative to the free surface.

The intensity diffracted from each element is spread over a range of 2θ angles due to instrumental and specimen broadening. The intensity due to all elements at each 2θ point is obtained by summing the individual contributions i.e.

$$P_B(2\theta) = I_o \sum_j Q_j \ \Delta V^g_{je} \ y_o \left[1 + \frac{(2\theta - 2\theta_j)^2}{ma^2} \right]^{-m} \tag{6}$$

where y_o is the normalization factor for the P-VII distribution[4] given in the brackets, and "a" and "m" are width and shape parameters respectively. Normalization requires

$$y_o = \frac{1}{a\sqrt{\pi m}} \frac{\Gamma(m)}{\Gamma(m - \frac{1}{2})}, \tag{7}$$

with $\Gamma(m) = \int_0^\infty x^{m-1} e^{-x} dx$ and $m > 0$. The full peak width w at 1/p of its maximum is related to shape and width parameters by

$$w\ (y_o/p) = 2a\ [m\ (p^{1/m} - 1)]^{1/2}. \tag{8}$$

The following rapidly converging series of error function complements ($\text{erfc}\ z = 1 - \text{erf}\ z$) was found to be very useful for curve fitting d-spacing profiles resulting from an atomic diffusion zone

$$d(Y) = d_o + \sum_{i=1}^{i=k} d_{1i}\ \text{erfc}\ (Y/d_{2i} - d_{3i}). \tag{9}$$

The spacing, d_o, is usually known for the substrate leaving only two terms or six constants required to curve fit the intensity bands from Ti-Aℓ samples. Setting $Y = 0$, gives $d(0)$ the spacing at the free surface. Allowing the argument $Y/d_{2i} - d_{3i}$ to be a large positive number for all terms, gives d_o as the required limit, for the undiffused substrate.

It is interesting to note that Eq. (9) can also be used to represent discontinuities in the d-spacing curve located at positions given by $Y_i = d_{2i}d_{3i}$. This becomes perceptible when d_{2i} becomes small relative to the element size ΔY_j. In the other extreme as $d_{2i} >> \Delta Y_j$, the corresponding erfc term becomes almost linear about its inflection point. These extreme variations in shape and the common occurence of the error function in solutions to the diffusion equation make Eq. (9) a useful expansion.

With the coefficients of Eq. (9) determined by visually fitting the experimental intensity points at a graphics terminal, the concentration profile $C(Y)$ is determined from the variation in the lattice parameters with composition.[6] In the present study, the lattice is based on α-Ti which is hexagonal and the conversion from $a(C)$ and $c(C)$ parameters to $d(C)$ is given by

$$\frac{1}{d^2} = \frac{4}{3}\left(\frac{h^2 + hk + k^2}{a^2}\right) + \frac{\ell^2}{c^2}.$$

which uniquely relates the d-spacing to composition. The (101) band of α-Ti is used because of its higher intensity.

EXPERIMENTAL RESULTS

Samples were prepared by sputtering either 1 or 0.5 μm Aℓ films onto 7/8" diam. x 1/8" thick Ti disks of 99.5% purity. The disks were cut from a Ti plate obtained from Semi-Alloys, Mount Vernon, N.Y. Preliminary diffusion anneals were carried out on the 1 μm samples at 635°C and examined after air cooling to room temperature. It was found that Aℓ reacts rapidly with Ti on the heat-up to 635°C forming a $Ti\,A\ell_3$ film at the surface. Beyond 4 hours, x-ray diffraction lines from Ti Aℓ become visible as the intensity from the $Ti\,A\ell_3$ phase diminished. During the early stage of diffusion, a weak but continuous intensity distribution was observed that extended from the $Ti_2A\ell$ composition to pure α-Ti. This is always on the high angle side of all α-Ti reflections and will be designated as the $Ti_3A\ell$/α-Ti intensity band.

After heating to 600°C and below, $Ti_8\,A\ell_{24}$ was observed along with $Ti\,A\ell_3$. This 2-phase structure was eliminated in favor of $Ti\,A\ell_3$ by rapid heating to 635°C as described in ref. (7). The preceeding reactions made use of as-prepared Aℓ/Ti samples.

With a 1 μm sample, it was found that when $Ti\,A\ell_3$/Ti is formed at 635°C and then heated to 900°C, the $Ti\,A\ell_3$ phase rapidly decomposes to give Ti Aℓ and $Ti_3\,A\ell$. After 15 minutes at 900°C, the intensity from the Ti Aℓ lines decreased while the intensity from the $Ti_3\,A\ell$ lines increased up to about 4 hours. Between 4 and 8 hours, the intensity from Ti Aℓ

decreased to zero and the intensity bands became more pronounced. At 8 hours, only Ti_3 Aℓ lines and relatively small α-Ti intensity bands are observable. The intensity bands grow rapidly after the Ti-Aℓ lines disappear. As will be seen later, this stage is relatable to the rapid release of Aℓ into α-Ti by the decomposition of the Ti_3 Aℓ phase.

When specimens containing 0.5 μm of Aℓ are used, the behavior on heating to 635°C for 2 hours is similar to that found with a 1 μm film after 8 hours. Heating to 900°C, in a two step process, gives a Ti_3 Aℓ overlayer at the surface. However, with these samples Ti Aℓ is not observed. Equilibrium in this system should be a homogeneous, single phase, dilute solution of Aℓ in α-Ti which is approached by the movement of the Ti_3 Aℓ/α-Ti interface toward the free surface, and concurrent release of Aℓ in α-Ti.

X-ray diffraction patterns for the (101) Ti_3 Aℓ/α-Ti intensity bands from a 1 μm Aℓ deposit are given in Fig. 1 for three diffusion times at 635°C. All patterns were obtained with monochromatic Cu $K_{\alpha 1}$ radiation and show a weak high angle intensity band that increased with diffusion time. The Ti $A\ell_3$ lines (not shown) are sharp and in accord with equilibrium diagrams giving this phase as a compound having very limited solubility. No other phases were observed after 1 hour at 635°C. However, after 2 hours, weak Ti Aℓ lines were observed and the release of Aℓ into α-Ti becomes retarded in the presence of this phase.

Figure 2 shows experimentally determined Aℓ-concentration profiles in an extended α-Ti solid solution obtained from the data in Fig. 1. An examination of Fig. 2 (b) and (c) shows a discontinuity in slope near 20% Aℓ in (b), which becomes a discontinuity in concentration in (c). This sequence of composition profiles illustrates that, in the initial

stage of diffusion at 635°C, Ti_3 Aℓ and α-Ti may be treated in terms of a single profile without a perceptable composition gap. With more diffusion time, a gap develops that correlates with the first appearance of lines from the Ti Aℓ phase. Even though a gap is not observed initially, the Ti_3 Aℓ (101) superlattice line is observed making Ti_3 Aℓ a separate phase distinguishable from disordered α-Ti. Both structures are based upon a hexagonal lattice, however, a_1 and a_2 must double in magnitude to describe the unit cell of Ti_3 Aℓ[8]. The (101) superlattice line contains much less composition broadening than the fundamental lines because the d-spacing profile is limited to the composition range of the Ti_3 Aℓ phase.

The simultaneous formation of a gap and the appearance of the Ti Aℓ phase after annealing at 635°C represents a step the system takes in approaching equilibrium. However, thin Aℓ deposits make it very difficult or impossible for all equilibrium phases to exist in perceptable amounts.

Figure 3 illustrates the rather unusual Cu $K_{\alpha 1}$ diffraction patterns that are obtained after annealing a 0.5 μm Aℓ film for 2 hours at 635°C and then ½, 1, and 4 hours at 900°C. These step anneals were carried out on three separate samples. The third peak at about 40.9° is associated with the Ti_3 Aℓ phase while the two at a lower angle correspond to the intensity band associated with the continuous composition profile in α-Ti. As one might expect, the intensity from the Ti_3 Aℓ phase decreases with time as does the low angle peak due to nearly pure Ti. The former is due to a decreasing amount of Ti_3 Aℓ and the latter results from absorption of the x-ray beam, because of the greater distance required to reach pure Ti as Aℓ diffuses into the substrate. The corresponding composition profiles are given in Fig. 4a, b and c. (Note the change in the distance scale between curves a and b).

The range of composition throughout each phase is of special interest. Within the α-Ti phase the composition limit is consistently at 20 at. % Aℓ (Figs. 2c and 4a, b and c) which is close to the 18 at. % value given by Margolin,[9] but greater than the 14% value given by van Loo et al.[7] and Kornilov et al.[10] The limit for the Ti_3 Aℓ phase is at about 34 at %. Margolin reported 38% and van Loo et al. 33%. The lower limit is at about 27 at. % (Figs. 4a, b, c) with 22% reported by Margolin et al. and 19% by van Loo. As one might expect, the interface compositions are not representative of the equilibrium values. Composition limits in this study are estimated to be within 3% for the Ti_3Aℓ phase and within 2% for disordered α-Ti.

The x-ray determinations of the composition profiles were in satisfactory agreement with Auger spectroscopy. Uncertainties in the ion milling rate and the uniformity of the milled cross section, introduce uncertainties in the depth axis of the composition profile. Despite these difficulties new information was obtained from Auger studies as well as from ESCA measurements that give a maximum Aℓ composition within the Ti_3 Aℓ phase of 29 at. % Aℓ. Although there was no apparent discontinuity at the Ti_3 Aℓ/α-Ti interface, there was a gradual transition in slope at a depth extending from 0.40 to 0.55 μm that is relatable to the interface. The composition in this region extends from 26 to 20% Aℓ. It is likely that a sharp discontinuity is not observed because of non-uniform ion milling near defects and smearing due to knock effects.

As new information, it was found that the oxygen concentration increases rapidly as the free surface is approached but this is localized to within 80A of the free surface. In going from about 80A to 1000A the Aℓ concentration increases from 22 to 29 at. % Aℓ. This small zone was not

predicted by x-ray diffraction. As a final point, the ESCA measurements at the free surface gave two oxide forms which were $A\ell_2O_3$ and TiO_2.

The data of Fig. 4 do not provide a determination of whether the interface moves parabolically or linearly with time. It has been shown that even when the interface movement is diffusion controlled, it need not move parabolically with time because of near surface affects. As a rough approximation, the thickness of $Ti_3A\ell$ decreased by about 0.2 μm/hr at 900°C.

DIFFUSION IN α-Ti (Aℓ)

A previously described[3] two-phase diffusion model was used to determine interdiffusion coefficients in the α-Ti (Aℓ) phase using 0.5 μm Aℓ samples. This model allows for a composition variation in the interdiffusion coefficient, a finite overlayer of Ti_3 Aℓ, and a semi-infinite substrate. Results are given in Fig. 5 for two temperatures. It is evident that good agreement is found at 900°C with van Loo et al.[7] However, composition variations were not treated by van Loo et al. Their analysis assumed the diffusion coefficient to be constant. A variation was observed in this study as is apparent in Fig. 5. At 635°C, the present data is about 3 to 10 times higher. Most of this discrepancy is likely to be due to differences in the defect structures of the samples employed. The data of van Loo et al. appeared to be less influenced by high diffusivity paths than the present samples.

Diffusion coefficients for the Ti_3 Aℓ phase tended to be an order of magnitude smaller than diffusion in the α-Ti(Aℓ) phase at 900°C. However, because of the limited solubility, these results are less reliable than the data reported for α-Ti (Aℓ). One might expect the ordered structure associated with Ti_3 Aℓ to give lower diffusion coefficients.[12]

ACKNOWLEDGEMENTS

The authors would like to acknowledge funding by the National Aeronautics and Space Administration (Langley Research Center), Grant #NSG-1470 and also Karl Wiedemann for obtaining Auger and ESCA data.

REFERENCES

1. V. B. Rao, C. R. Houska, J. Unnam, W. D. Brewer, and D. R. Tenney: New Developments and Applications in Composites, D. Kuhlmann - Wilsdorf and W. C. Harrigan, Jr., Eds., p. 347-359, The Metallurgical Society of AIME, 1980.
2. C. R. Houska: Treatise on Materials Science, H. Herman, Ed., Vol. 19A, pp. 63-105, Academic Press, Inc., NY, 1980.
3. J. Unnam, and C. R. Houska: J. Appl. Phys., 1976, Vol. 47, pp. 4336-42.
4. M. M. Hall, V. G. Veeraraghaven, H. Rubin, and P. G. Winchell: J. Appl. Cryst., 1977, Vol. 10, pp. 66-68.
5. B. D. Cullity: Elements of X-Ray Diffraction, Addison-Wesley, MA, 1978, pp. 408 and 183.
6. D. Clark, K. S. Jepson, and G. I. Lewis: J. Inst. Met., 1962, Vol. 91, p. 11.
7. F. J. J. van Loo and G. D. Rieck: Acta Met., 1973, Vol. 21, pp. 61-71.
8. W. B. Pearson: Handbook of Lattice Spacings and Structures of Metals, pp. 41, 133, 342 and 599, Pergammon Press, NY, 1967.
9. H. Margolin: Metals Handbook, T. Lyman, Ed., Vol. 8, p. 264, American Society for Metals, Metals Park, Ohio, 1973.
10. I. I. Kornilov, T. T. Nartora and S. P. Chernyshova: Russian Metallurgy (Translation), 1976, No. 6, p. 156.
11. J. Goold: J. Inst. Met., 1959, Vol. 88, p. 444.
12. Augusto Penaloza and C. R. Houska, "Refinements on the X-Ray Intensities from $Ti_{3-2}A\ell$," submitted to Met. Trans. 1982.

Figure Captions

Fig. 1. (101) Ti_3Al/α-Ti x-ray intensity bands from a 1 μm Al/α-Ti sample diffused for 0.5, 1.0, 2.0 hrs at 635°C. All data were obtained with Cu $K_{\alpha 1}$ radiation.

Fig. 2. Al concentration profiles obtained from intensity band data of Fig. 1 for 0.5, 1.0, and 1.5 hrs at 635°C.

Fig. 3. (101) Ti_3Al/α-Ti intensity bands from a 0.5 μm Al/α-Ti sample first reacted at 635°C for 2 hrs and then 0.5, 1.0, and 4.0 hrs at 900°C. All data were obtained with Cu $K_{\alpha 1}$ radiation.

Fig. 4. Al concentration profiles obtained from intensity bands of Fig. 3 for 0.5, 1.0, and 4.0 hrs at 900°C after 2 hrs at 635°C.

Fig. 5. Interdiffusion coefficients for the diffusion of Al in α-Ti. The present data obtained at 900 and 635°C are compared with results published by (1) Goold[11] and (2) van Loo and Rieck.[7]

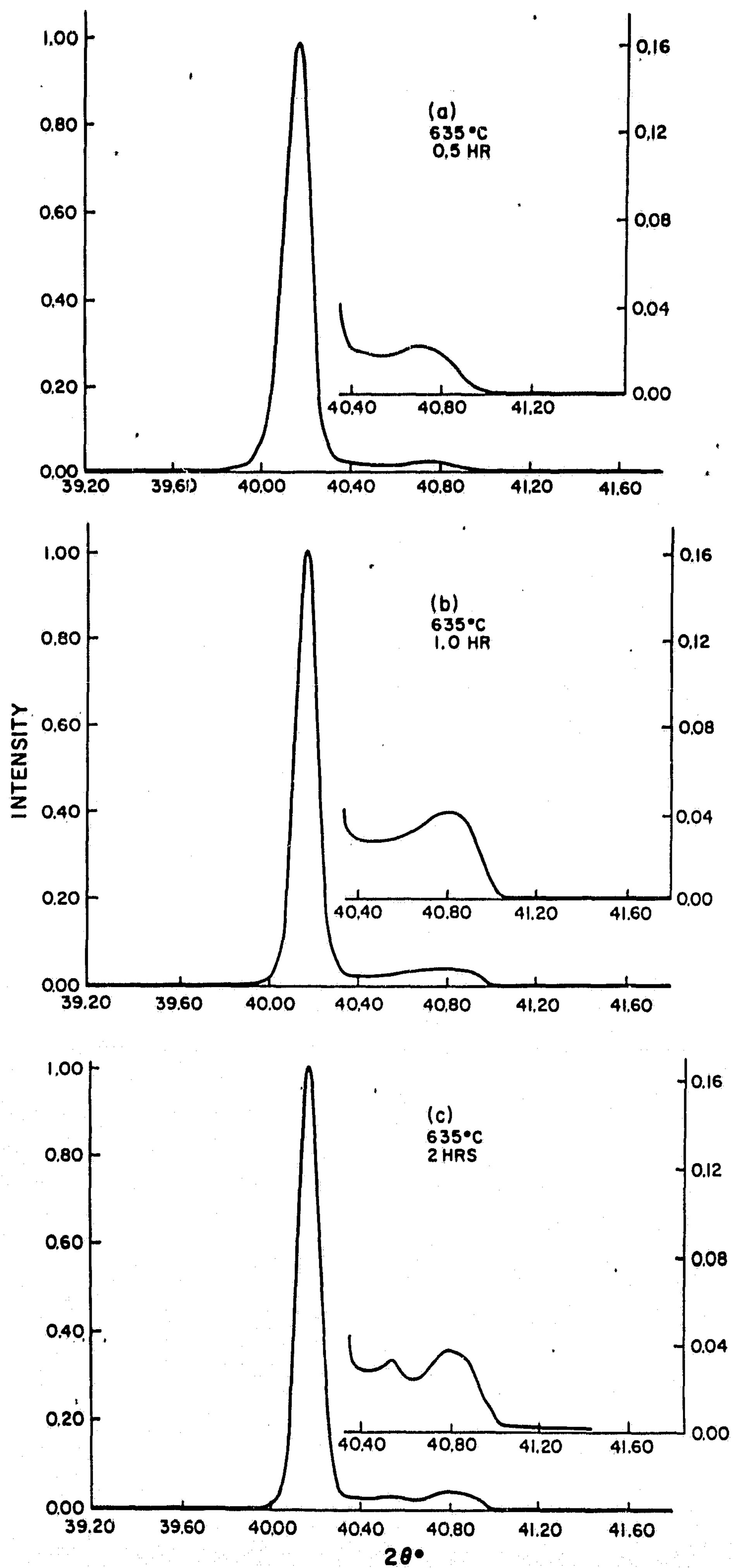

Fig. 1

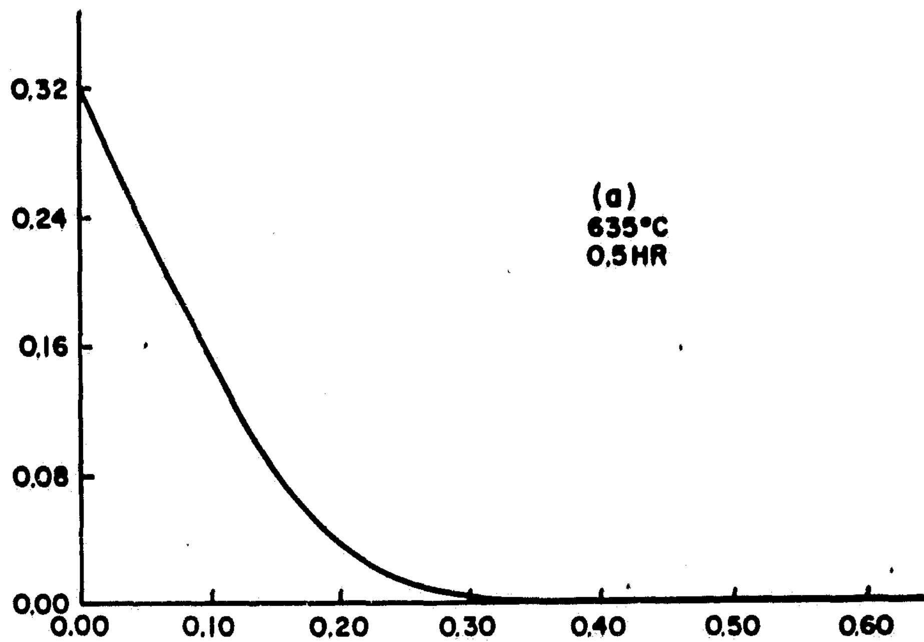

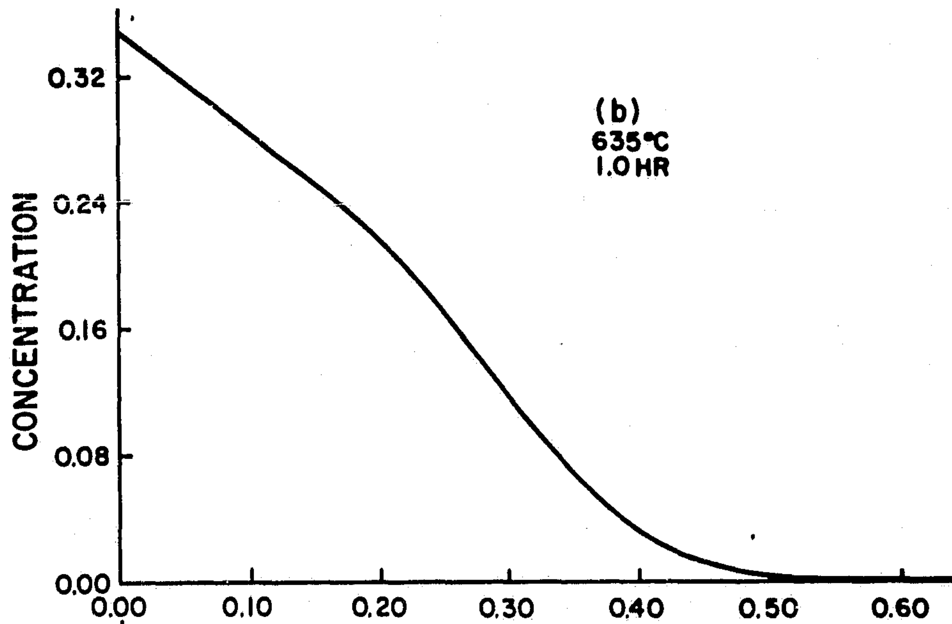

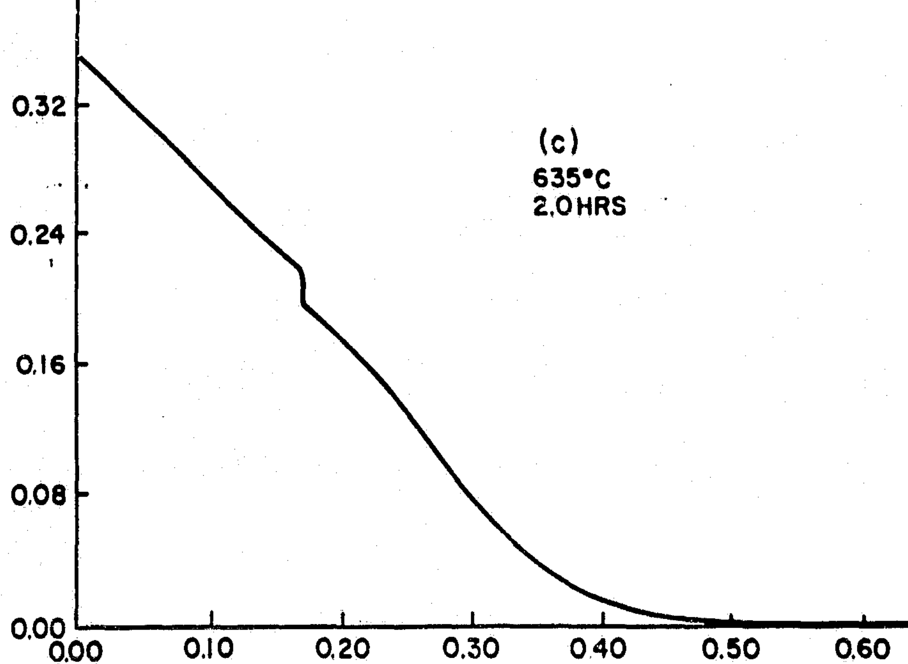

Fig. 2

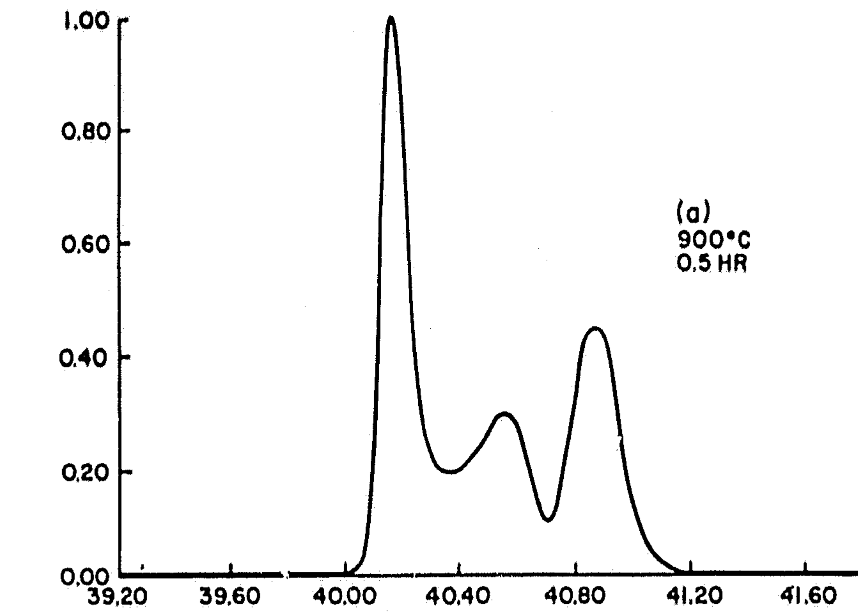

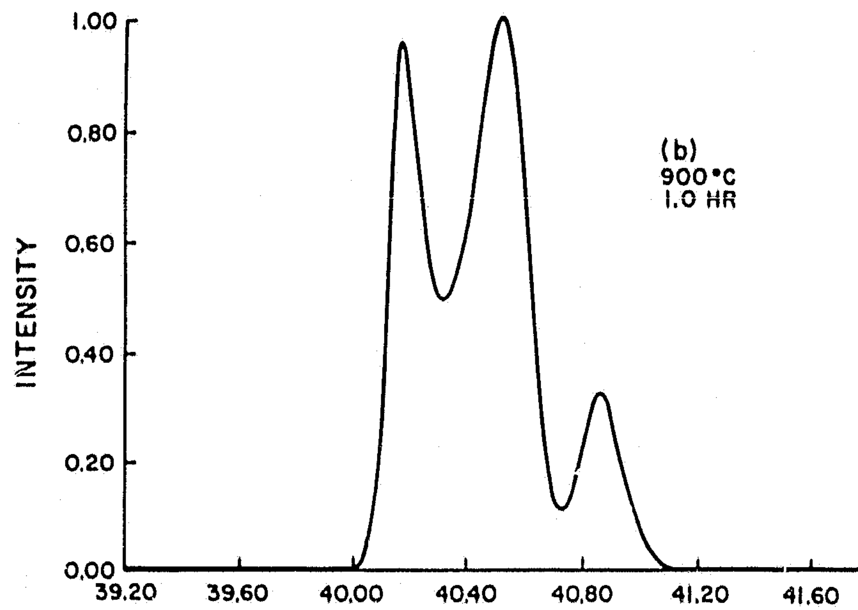

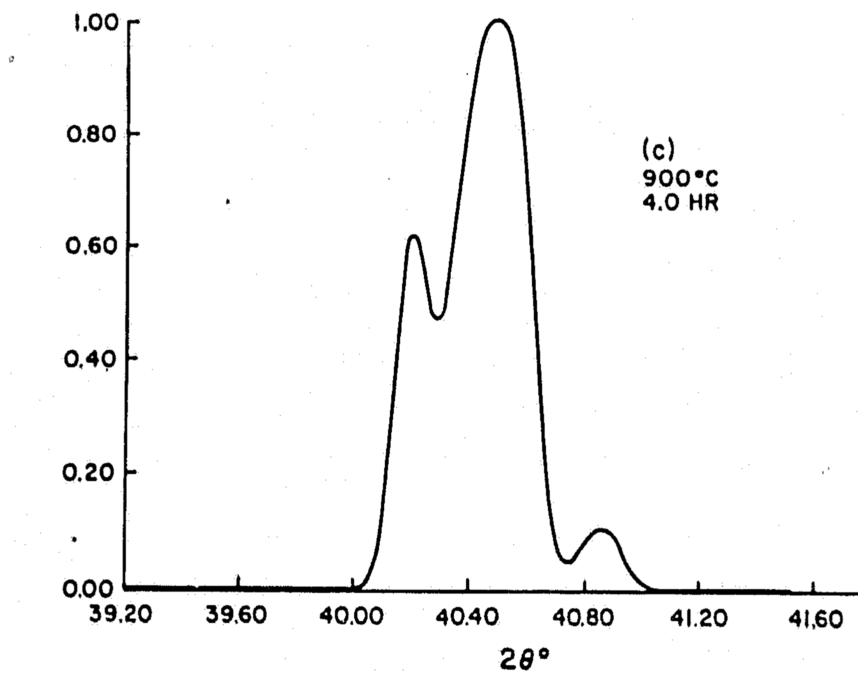

Fig. 3

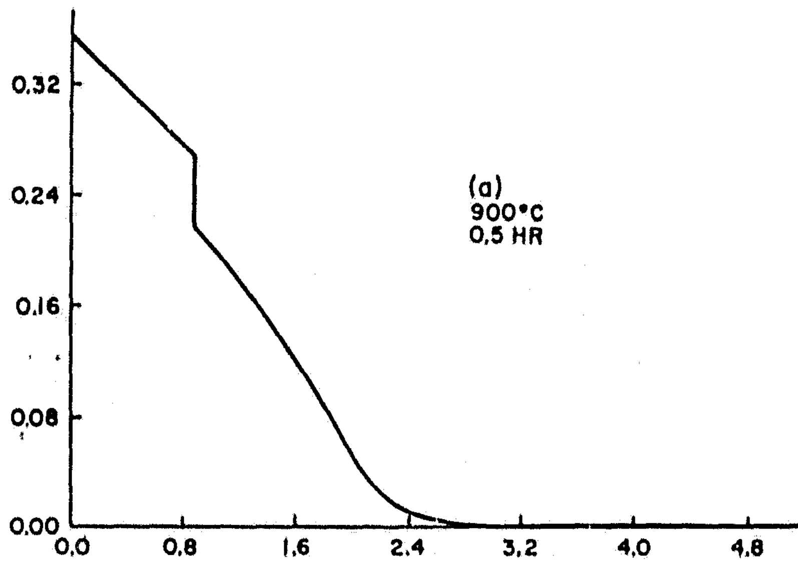

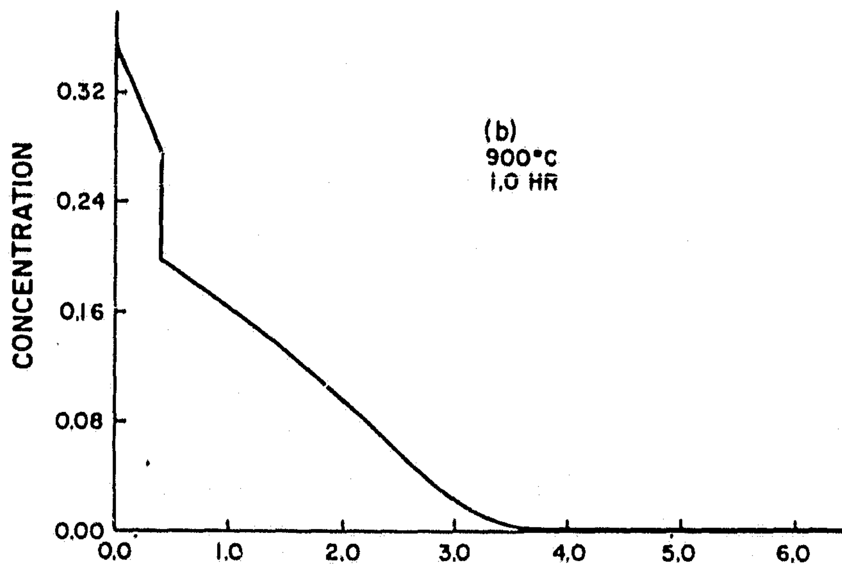

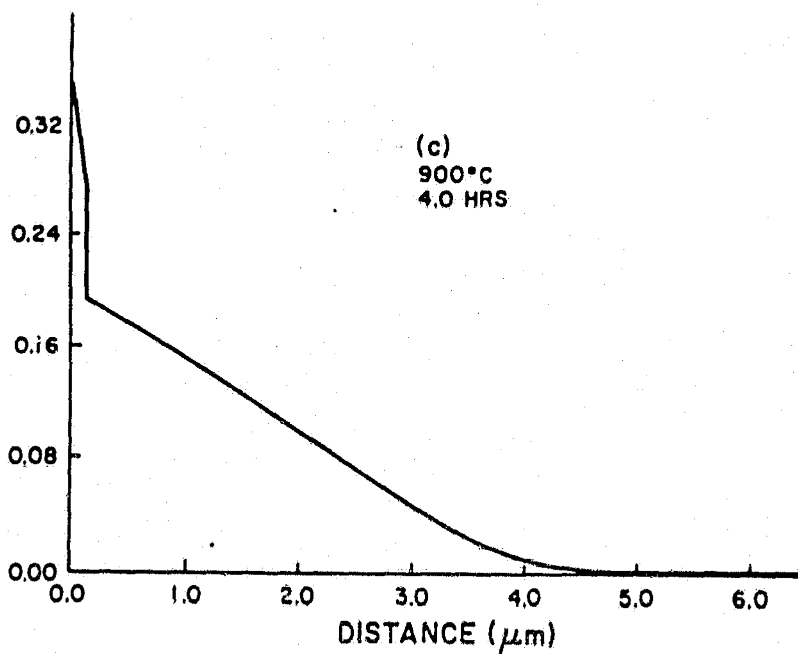

Fig. 4

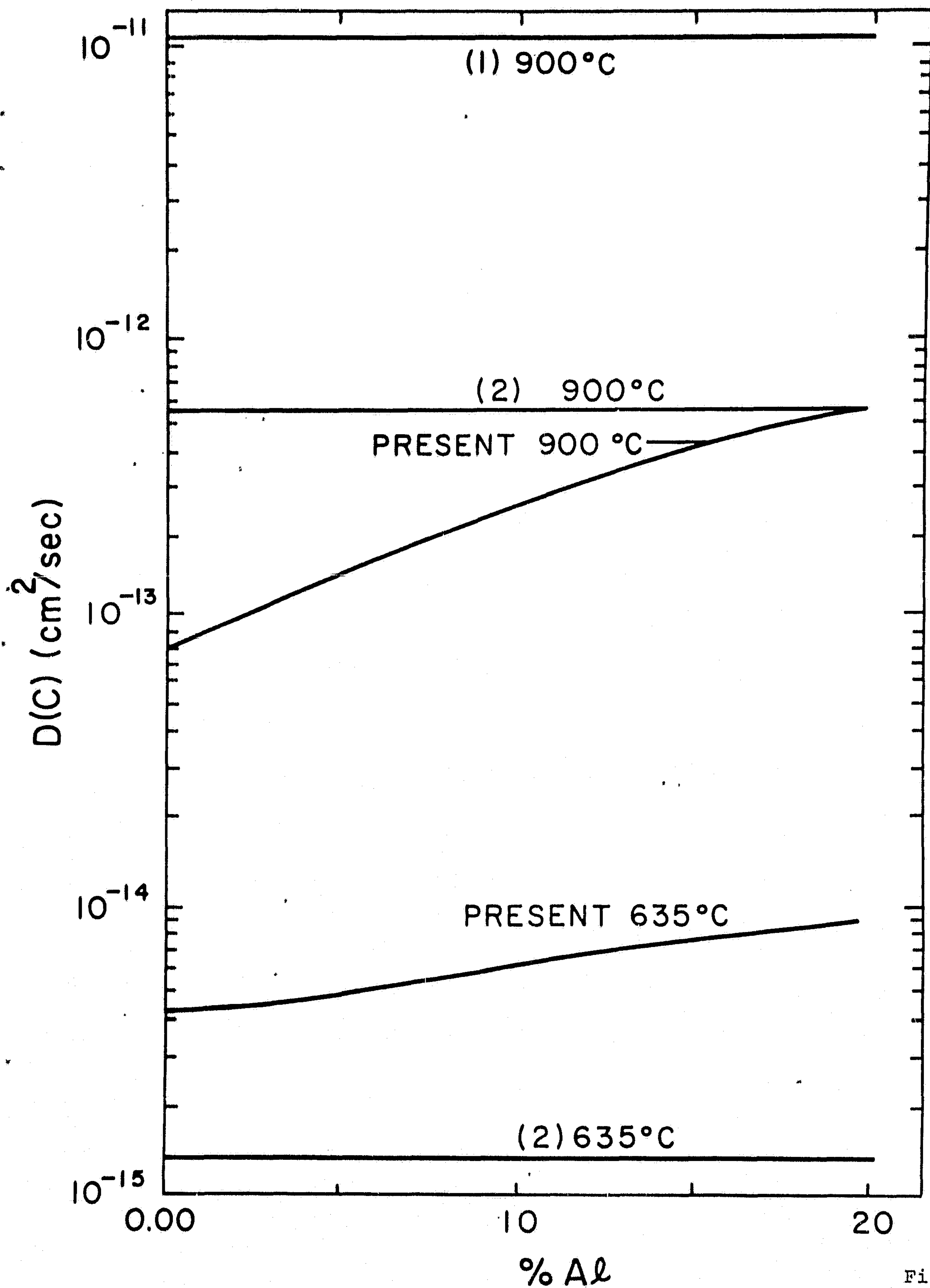

Fig. 5

Refinements on the X-Ray Intensities From Ti_{3-2} Aℓ

Augusto Penaloza and C. R. Houska

As a result of a recent x-ray study[1] of diffusion between an Aℓ film and Ti substrate, it was discovered that an explicit intensity expression for the intermetallic Ti_{3-2} Aℓ phase has not been given. This has created some confusion as to the various classes of reflections that are found for this phase. Also, eight superlattice lines were observed using a diffracted beam graphite monochromator and a high intensity fine focus x-ray tube as compared with only two from an earlier work.[2] These contributions are included in this technical note and provide stronger evidence that the structure of Ti_3 Aℓ is of the Ni_3 Sn type.

A sample containing 28% Aℓ was prepared by vacuum annealing a mixture of 325 mesh powders with Ti (99% pure) and Aℓ (99.8% pure) both obtained from Alfa-Ventron Division (Danvers, Mass.). Annealing was carried out in a quartz tube containing an alundum boat at $3X10^{-6}$ torr using ion and sorption pumping. The mixed powder was first reacted for 8 hours at 635°C and then for 7 days at 900°C after which the quartz tube was air cooled to room temperature in about 3 hours. The sintered powder was crushed to < 325 mesh for an x-ray diffraction sample.

Augusto Penaloza is Assistant Professor, Physics Department, Catholic University of Valparaiso, Chile, and C. R. Houska is Professor, Department of Materials Engineering, Virginia Polytechnic Institute and State University, Blacksburg, VA 24061-2898.

Intensities were obtained by measuring the areas above background with a planimeter. Overlapping lines were separated by least squares fitting with a Pearson VII function. When the lines were well separated, the positions were obtained with the peak bisection method.

The relative integrated intensities are given by

$$I \approx p \frac{1 + \cos^2 2\theta \cos^2 2\alpha}{(1 + \cos^2 2\alpha) \sin\theta \sin 2\theta} |F|^2 \quad (1)$$

where p is the multiplicity, θ and α are the diffraction angles of the sample and monochromator ($\alpha \approx 26°$ for graphite). Pearson[3] has listed that the $Ti_{3-2}A\ell$ phase is hexagonal and of the Ni_3Sn type, with space group P 6_3/mmc having

6 - Ti in h at: $x, 2x, \frac{1}{4}; 2\bar{x}, \bar{x}, \frac{1}{4}; x, \bar{x}, \frac{1}{4}; \bar{x}, 2\bar{x}, \frac{3}{4}; 2x, x, \frac{3}{4}, \bar{x}, x, \frac{3}{4}$

2 - Aℓ in c at: $\frac{1}{3}, \frac{2}{3}, \frac{1}{4}; \frac{2}{3}, \frac{1}{3}, \frac{3}{4}$

and x = 5/6. The structure factor may be most conveniently written as

$$F = f_{A\ell} S_c + \langle f \rangle_h S_h \quad (2)$$

where $f_{A\ell}$ and $\langle f \rangle_h$ are the scattering factors for Aℓ and position "h" respectively. The latter scattering factor represents an average due to a random mixing of Ti and excess Aℓ atoms in position "h". For stoichiometric $Ti_3 A\ell$ all c and h positions are occupied by Aℓ and Ti respectively. As the $Ti_2 A\ell$ composition is approached, the c positions remain occupied entirely by Aℓ while the excess Aℓ atoms combine with Ti to fill the h positions. The symmetry factors S_c and S_h for the equipoint sets c and h depend only upon the atomic positions in the unit cell and are independent of the atom type.[4] The composition limit on the

low Aℓ side has been reported to be in the range between 18 to 22 at. % Aℓ.[5-7] In this range, it is assumed that the excess Ti occupies c positions at random with Aℓ and that h positions are completely filled with Ti giving

$$F = \langle f \rangle_c S_c + f_{Ti} S_h. \qquad (2')$$

Useful calculations of symmetry factors are available in ref. 8, p. 489. Simplified forms are given in Table I where X_{Ti} and $X_{A\ell}$ are the atomic fractions of Ti and Aℓ. It can be seen that there are four classifications for the fundamental lines and the same number designated as superlattice lines. The (a) (b) listings are arranged in terms of decreasing magnitude of the structure factor. It should be noted that F II(b) and S II(b) correspond to F = 0.

The measured reflections are separated into their respective classes in Table II. This table includes observed d-spacings, relative intensities and three sets of calculations based on Ti_3 Aℓ, Ti_2 Aℓ, and Ti(0.78) Aℓ(0.22) using previously reported lattice parameters.[9] The latter entry corresponds to a limiting solubility on the Ti rich side. All calculations are based upon the most recent atomic scattering factors.[10] The differences in intensities relative to Ti_3 Aℓ are very small when compared with a maximum value of 100 and become insignificant when other experimental difficulties are considered. The differences in d-spacings are readily, measured and represent the best way to distinguish composition changes in this system by x-ray diffraction. When the degree of discrepancy between the experimental data and the Ni_3 Sn type structure for Ti_3 Aℓ is calculated using

$$R = \frac{\sum |F| - |F_e|}{\sum |F|},$$

one obtains R = 0.12. This value has been increased somewhat by a preferred orientation of (00ℓ) planes within the present sample. This, of course, gives larger values for the (002) and (004) reflections. The lattice parameters were found to be a = 5.780 A and c = 4.647A with standard deviations of 0.003A and 0.006A respectively.

The authors would like to acknowledge funding by the National Aeronautics and Space Administration (Langley Research Center), Coop. Agree. #NCCI-10 and computer assistance from Karl Wiedemann.

References

1. V. Rao and C. R. Houska: Reactions and Diffusion Between an Aℓ Film and a Ti substrate (submitted to Met. Trans. A.).

2. A. J. Goldak and J. Gordon Parr: Trans. AIME, 1961, Vol. 221, p. 639.

3. W. B. Pearson: Handbook of Lattice Spacings and Structures of Metals, pp. 41, 133, 342 and 599, Pergammon Press, NY, 1967.

4. L. V. Azaroff: Elements of X-Ray Crystallography, p. 286, McGraw-Hill, NY, 1968.

5. P. A. Farrar and H. Margolin: Air Force Materials Lab. Tech. Rept. AFML-TR-65-69, 1965.

6. F. J. J. van Loo and G. D. Rieck: Acta Met., 1973, Vol. 21, p. 61.

7. I. I. Kornilov, T. T. Nartova, and S. P. Chernyshova: Russian Metallurgy (Translation), 1976, No. 6, p. 156.

8. N. F. M. Henry and K. Lindsdale: International Tables for X-Ray Crystallography, Vol. 1, Symmetry Groups, pp. 304 and 489, Kynoch Press, Birmingham, Eng., 1969.

9. D. Clark, K. S. Jepson, and G. I. Lewis: J. Inst. Met., 1962, Vol. 91, p. 11.

10. J. A. Ibers and W. C. Hamilton: International Tables for X-Ray Crystallography, Vol. IV, Revised and Supplementary Tables to Vol. II and III, Kynoch Press, Birmingham, Eng., p. 99.

Table I - Structure factors for the $Ti_3A\ell$ phase

Fundamental Lines (h and k are even)

F I, ℓ = Even

(a) $h + 2k = 3n$, $F^2 = 64 \langle f \rangle^2$

(b) $h + 2k = 3n \pm 1$, $F^2 = 16 \langle f \rangle^2$

F II, ℓ = Odd

(a) $h + 2k = 3n \pm 1$, $F^2 = 48 \langle f \rangle^2$

(b) $h + 2k = 3n$, $F^2 = 0$

Superlattice Lines (one or both h and k are odd)

S I, ℓ = Even

(a) $h + 2k = 3n$, $\begin{cases} F^2 = \frac{64}{9} X_{Ti}^2 (f_{Ti}-f_{A\ell})^2, & \frac{3}{4} \geq X_{Ti} \geq \frac{2}{3} \\ F^2 = 64\, X_{A\ell}^2 (f_{Ti}-f_{A\ell})^2, & \frac{1}{4} \geq X_{A\ell} \end{cases}$

(b) $h + 2k = 3n \pm 1$, $\begin{cases} F^2 = \frac{16}{9} X_{Ti}^2 (f_{Ti}-f_{A\ell})^2, & \frac{3}{4} \geq X_{Ti} \geq \frac{2}{3} \\ F^2 = 16\, X_{A\ell}^2 (f_{Ti}-f_{A\ell})^2, & \frac{1}{4} \geq X_{A\ell} \end{cases}$

S II, ℓ = Odd

(a) $h + 2k = 3n \pm 1$, $\begin{cases} F^2 = \frac{48}{9} X_{Ti}^2 (f_{Ti}-f_{A\ell})^2, & \frac{3}{4} \geq X_{Ti} \geq \frac{2}{3} \\ F^2 = 48\, X_{A\ell}^2 (f_{Ti}-f_{A\ell})^2, & \frac{1}{4} \geq X_{A\ell} \end{cases}$

(b) $h + 2k = 3n$, $F^2 = 0$

Table II An intercomparison of relative intensities and d-spacings at three compositions. 3+ corresponds to Ti(0.78) Aℓ(0.22)

hkℓ Type													
F I a	F I b	F II a	S I a	S I b	S II a	d_{obs}	d_2	d_3	d_{3+}	$(\frac{I}{I_o})_{obs}$	$(\frac{I}{I_o})_2$	$(\frac{I}{I_o})_3$	$(\frac{I}{I_o})_{3+}$
				100		5.003	4.998	5.019	5.027	1.9	1.7	2.2	1.6
					101	3.405	3.398	3.410	3.414	5.1	4.0	5.1	3.8
			110			2.890	2.886	2.898	2.902	1.2	1.7	2.2	1.6
	200					2.503	2.499	2.510	2.513	23.1	24.5	24.6	24.6
002						2.325	2.316	2.324	2.326	(45.8)	26.1	26.0	26.0
		201				2.204	2.199	2.208	2.211	100.0	100.0	100.0	100.0
				210		1.892	1.889	1.897	1.900	0.5	0.2	0.3	0.2
			112			1.810	1.806	1.813	1.815	1.0	0.7	0.9	0.7
					211	1.750	1.749	1.756	1.759	0.8	1.0	1.2	0.9
	202					1.702	1.699	1.705	1.707	15.7	14.3	14.2	14.2
					103	1.478	1.475	1.480	1.482	0.4	0.2	0.3	0.2
220						1.445	1.443	1.449	1.451	15.0	16.1	16.0	16.0
			302			1.354	1.352	1.358	1.360	0.4	0.2	0.3	0.2
		203				1.318	1.314	1.318	1.320	21.0	17.4	17.2	17.1
	400					1.251	1.249	1.255	1.257	2.0	2.4	2.4	2.4
222						1.227	1.225	1.230	1.231	18.4	18.2	17.9	17.9
		401				1.208	1.206	1.211	1.213	15.5	13.0	12.8	12.8
004						1.163	1.158	1.162	1.163	(4.1)	2.5	2.5	2.5
	402					1.102	1.100	1.104	1.106	2.1	3.3	3.2	3.2
	204					1.053	1.051	1.054	1.056	2.1	2.9	2.9	2.9
		403				0.9733	0.9713	.9751	.9763	5.6	7.8	7.6	7.6
	420					0.9456	0.9445	.9486	.9500	1.3	2.5	2.5	2.5
		421				0.9265	0.9255	.9294	.9308	12.6	15.2	14.9	14.8
224						0.9054	0.9031	.9064	.9075	8.6	10.3	10.0	9.9
	422					0.8760	0.8746	.8782	.8794	5.2	5.4	5.2	5.2
		205				0.8714	0.8687	.8716	.8726	6.3	8.2	8.0	7.9
	404					0.8513	0.8494	.8525	.8536	1.7	2.9	2.8	2.8
600						0.8343	0.8330	.8366	.8378	2.8	6.3	6.1	6.0
		423				0.8071	0.8058	.8090	.8101	16.8	24.1	22.9	22.5